Resonant Raman scattering by plasmons and LO phonons near the E_1 and $E_1+\Delta_1$ gaps of GaSb

Wolfgang Kauschke, Narcís Mestres, and Manuel Cardona
Max-Planck-Institut für Festkörperforschung, Heisenbergstrasse 1, D-7000 Stuttgart 80, Federal Republic of Germany
(Received 30 April 1987)

We report on the resonance of Raman scattering by plasmons near the E_1 and $E_1+\Delta_1$ gaps of heavily doped n-type GaSb. The dipole-allowed Raman scattering by plasmons due to the electro-optic (Fröhlich interband) coupling of bands interferes with the dipole-forbidden **q**-dependent Fröhlich intraband scattering. Absolute values of Raman polarizabilities and efficiencies are displayed. The interference is compared with that of the LO phonons seen from the surface depletion layer. Theoretical expression for the resonance of the different scattering mechanisms (electro-optic, Fröhlich intraband, electric field induced, deformation potential, impurity induced, 2LO) near the E_1 and $E_1+\Delta_1$ gaps are derived and compared with the experiment. The dispersion of the second-order susceptibility $\chi^{(2)}_{123}(\omega_L,-\Omega_P,\omega_S)$ is displayed and the Faust-Henry coefficient of GaSb determined.

I. INTRODUCTION

Interference effects near the $E_0+\Delta_0$ gap of III-V compounds between dipole-allowed deformation-potential scattering and dipole-forbidden Fröhlich intraband **q**-dependent Raman scattering by LO phonons are an established phenomenon [GaAs,[1–4] InP,[5] GaSb,[6] GaP (Ref. 7)]. They can be described by a theory which assumes uncorrelated electron-hole pairs as intermediate states. Interference effects have also been reported for LO phonons near the E_1 gap of InSb and have been successfully explained by the theory.[8]

Interference effects in Raman scattering by the coupled longitudinal-optical-phonon–plasmon modes of n-type GaAs ($n=1\times10^{18}$ cm^{-3}) near the $E_0+\Delta_0$ gap were observed by Chen.[9] For the interpretation of these data, deformation-potential, electro-optic (Fröhlich interband), and **q**-dependent (Fröhlich intraband) scattering and charge-density fluctuations must be considered.[10–14] Near the E_1 and $E_1+\Delta_1$ gaps no free carriers are present in direct-gap semiconductors, thus the charge-density fluctuation mechanism is not operative.

The first observation of coupled LO-phonon–plasmon modes in Raman spectra excited with photon energies near the E_1 gap was reported by Buchner and Burstein.[15] The measurements were carried out in accumulation space-charge layers at (100) surfaces of n-type InAs. The E_1 gap of GaSb ($\cong$2.16 eV) (Ref. 16) is easily accessible with cw dye lasers, and in highly n-doped samples ($n\gtrsim10^{18}$ cm^{-3}) the L_+ modes are almost plasmonlike, corresponding to pure electron-plasma oscillations, whereas the frequency of the L_- mode nearly coincides with that of the TO phonon (screened LO phonon).[12,13,17–21] Thus the two particles decouple: only Raman scattering mechanisms associated with their internal electric fields must be considered for the plasmons. The electric field of the plasmon couples *interband* via the Fröhlich electron-plasmon interaction, and yields the electro-optic scattering which obeys the usual dipole-selection rules.[13,22] The mechanism corresponds to a three-wave mixing of the electric fields of the incident photon, plasmon, and scattered photon, and is closely related to the nonlinear optical response.[23–25] The *intraband* matrix elements of the Fröhlich interaction give the usual dipole-forbidden, **q**-dependent Fröhlich-induced scattering.[26] Both mechanisms lead to the same final state (**q** is fixed by the optical scattering vector): they are mutually coherent and can interfere. Incoherent mechanisms, like impurity-induced scattering in the case of LO phonons,[2,27] should be weak, since the impurity potential is strongly screened by the electron plasma. Thus we expect similar interference effects for Raman scattering by plasmons near the E_1 and $E_1+\Delta_1$ gaps as for LO phonons in undoped material, except for the incoherent contribution to the scattering intensity.

On the other hand, polar semiconductors are known to possess surface depletion or enrichment layers (for n-type GaSb depletion layers).[28–30] Near the E_1 gap, the penetration depth of the light is of the order of the layer thickness ($1/2\alpha\cong$100–200 Å) for $n\gtrsim10^{18}$ cm^{-3} in GaSb: both features, the coupled modes L_+ and L_- from the bulk, as well as the LO phonon from the surface depletion layer, are seen in the Raman spectra.[20,29,30] The measurement of the interference effects of plasmons near the E_1 and $E_1+\Delta_1$ gaps yields the possibility of comparing plasmon and LO-phonon resonances; absorption corrections, however, are important and delicate. The thickness of the depletion layer can be determined rather accurately with Raman scattering by comparing the intensities of the LO phonon and screened LO phonon for different laser energies (penetration depths of the light).[30]

Several scattering mechanisms resonant near the E_1 and $E_1+\Delta_1$ gaps must be taken into account for the LO phonon. They have been reviewed by Richter *et al.*[31] and Menéndez *et al.*[8] There are two-band and three-band contributions to the deformation-potential dipole-allowed scattering by LO phonons and the standard

Fröhlich intraband dipole-forbidden scattering. The Fröhlich interband or electro-optic mechanism is usually assumed to be a small correction to deformation-potential scattering. It gives rise to small differences in Raman scattering efficiencies between LO and TO phonons.[12,22] An additional dipole-forbidden scattering mechanism induced by the surface electric field has been proposed by Pinczuk and Burstein.[32] It is formally similar to the Fröhlich **q**-dependent Raman scattering and becomes important at fields of the order of 10^4 V/cm.[32,33] The impurity-induced dipole-forbidden Raman scattering by LO phonons proposed by Gogolin and Rashba[27] has also been shown to be operative near the E_1 and $E_1+\Delta_1$ gaps: In this case the uncorrelated electron-hole pair, labeled here as the exciton, is scattered twice, by the LO phonon via the Fröhlich electron-phonon interaction, and elastically by the impurity.[2] In this fourth-order process the **q** conservation is relaxed and the whole LO-phonon branch can be activated. The 2LO-phonon scattering is formally equivalent to the impurity-induced Raman scattering by LO phonons: A second Fröhlich electron-phonon interaction replaces the electron-impurity interaction.[34–36] Although some resonance Raman data of LO phonons are available for the E_1 or $E_1+\Delta_1$ gaps of GaAs,[37] GaSb,[38,39] InAs,[40] or InSb (Refs. 8,31,38, and 41), the resonance of impurity-induced and 2LO-phonon scattering derived from the **q** dependence of the Fröhlich interaction have so far not been calculated for the two-dimensional E_1 gap. Here we present such calculations and compare them with new experimental data. As far as the intrinsic first-order Raman scattering mechanisms by LO phonons are concerned, we reformulate the calculations of Ref. 31 in order to derive the correct prefactors and signs for the corresponding effect of the plasmons.

II. EXPERIMENTAL

The GaSb samples studied were cut with a (001) face from a Czochralski-grown tellurium-doped ingot ($n\cong N_d=2\times10^{18}$ cm^{-3}). The Raman spectra show the LO-phonon–plasmon coupled modes L_+ and L_- (Refs. 12–14) as well as the unscreened LO phonon from the surface depletion layer.[28,30] We may consider the L_+ mode as a *pure* plasmon, since the phonon admixture to the L_+ mode is negligible at $n\cong2\times10^{18}$ cm^{-3} ($\hbar\Omega_P=75$ meV). The frequency of the L_- mode (screened LO phonon) nearly coincides with that of the TO phonon, which lies very close to the LO phonon ($\hbar\Omega_-\cong29$ meV, $\hbar\Omega_{LO}\cong30$ meV). Neither feature was resolved over the whole spectral range under investigation ($\hbar\omega_L=1.9-2.7$ eV) by the optical multichannel detection system used.

The absorption of the material varies strongly with energy close to the E_1 and $E_1+\Delta_1$ gaps, thus requiring corrections for the Raman scattering efficiencies. The absorption of the sample was determined by spectroscopic ellipsometry at 30 K. The measured complex reflectance ratio $\rho=r_p/r_s$ was analyzed within the three-phase model of the sample (air-oxide-substrate).[42] The values of the dielectric function of the oxide layer on GaSb were taken from the literature.[43] Its thickness was determined to be 36 Å. From the resulting complex dielectric function for the substrate, the absorption coefficient, the refractive index, and the reflectivity of the heavily doped GaSb were calculated as a function of energy.[44]

By performing a line-shape analysis of the spectrum of the second derivative of the complex dielectric function with respect to the photon energy, $\hbar^{-2}d^2\epsilon/d\omega^2$, the parameters of the E_1 and $E_1+\Delta_1$ critical points (energy, width, amplitude, phase angle) were determined.[45,46]

The optical susceptibility χ ($\epsilon=1+4\pi\chi$) can be decomposed into contributions from the E_1 (χ^+) and $E_1+\Delta_1$ (χ^-) critical points. Due to the very large longitudinal mass in the [111] direction with respect to the transverse one, the E_1 and $E_1+\Delta_1$ critical points can be assumed to be two dimensional. Then the susceptibilities $\chi^\pm$ are approximately given by[8,45,46]

$$\chi^+(E)=-\frac{A^+e^{i\phi^+}}{E^2}(E_1+\Delta_1/3)\ln(1-x_1^2) \tag{1}$$

and

$$\chi^-(E)=-\frac{A^-e^{i\phi^-}}{E^2}(E_1+2\Delta_1/3)\ln(1-x_{1s}^2)\ . \tag{2}$$

x_1, and x_{1s} are "reduced" energies defined as $x_1=E/(E_1-i\eta^+)$, and $x_{1s}=E/(E_1+\Delta_1-i\eta^-)$, where $\eta^\pm$ denote the broadening of the corresponding gaps. $A^\pm$ are the (real) amplitudes of the critical points and $\phi^\pm$ are the phase angles which describe phenomenologically excitonic effects on the E_1, $E_1+\Delta_1$ transitions ($\phi=0$ for a pure two-dimensional (2D) interband minimum, $\phi=\pi/2$ for a 2D saddle point).[46] $E_1=2.160$ eV, $\eta^+=29.2$ meV, $A^+=0.54$ eV and $E_1+\Delta_1=2.597$ eV, $\eta^-=40.8$ meV, $A^-=0.54$ eV were obtained from the line-shape analysis of the ellipsometric data with $\phi^+=\phi^-\cong119°$. From $\mathbf{k}\cdot\mathbf{p}$ expressions one obtains $A^+\cong A^-\cong4\sqrt{3}e^2/9\pi a_0=0.57$ eV with e the free-electron charge and a_0 the lattice constant.[45]

The Raman measurements were performed in backscattering geometry in a helium-flow cryostat at about 10 K. For the excitation of spectra we used the discrete lines of Kr^+- and Ar^+-ion lasers as well as a cw dye laser with R6G (Lambda Physik, Göttingen) pumped by all lines of an Ar^+ laser (5 W) and with Coumarin 6 (Lambda Physik, Göttingen) pumped by the 488-nm line of an Ar^+ laser (3 W). The dye lasers covered the spectral range 1.93–2.35 eV, close to the E_1 gap of GaSb. The laser beam was focused with a cylindrical lens onto the sample in order to keep the power density below 10 W/cm^2.

The notation of the coordinate axes is that of Ref. 2. We denote by x, y, z, x', and y' the [100], [010], [001], [110], and [$\bar{1}$10] directions, respectively. We choose the Ga atom at the origin and the Sb atom at a $(a_0/4)$ (1,1,1). With this convention the ($\bar{1}1\bar{1}$) plane (parallel to [110] is Ga terminated. The [110] and [$\bar{1}$10] directions are physically inequivalent on a (001) surface and can be distinguished by inspection of the etch pattern produced

by preferential etching with a $0.2M$ solution of $Fe_2(SO_4)_3$ in 37% HCl.[47]

The Raman measurements were performed in four different backscattering configurations which, in the case of Raman scattering by LO phonons, allow us to distinguish between the dipole-allowed and dipole-forbidden contributions as well as to measure their interference: $\bar{z}(x',x')z$ (I), $\bar{z}(y',y')z$ (II), $\bar{z}(x,x)z$ (III), and $\bar{z}(y,x)z$ (IV).[1-8] The spectra were analyzed with an optical multichannel analyzer (OMA) system composed on a triplemate monochromator (Spex Industries, Metuchen, NJ) and a position-sensitive photomultiplier (Mepsicron F4146M, ITT, Fort Wayne, IN).[48] The resolution of our spectrometer was about 3 Å for the 1200-line/mm grating-monochromator stage, essentially limited by the cross talk between two neighboring "channels" of the channel plate (extending about five channels). Thus we were not able to resolve the L_- mode from the LO-phonon line over the whole spectral range under investigation. The common feature will be labeled "LO."

We used the sample-substitution method to obtain absolute values for the Raman tensor.[22] High-purity silicon served as a reference ($|a|_{Si}=70\pm30$ Å^2 at $\hbar\omega_L=2.2$ eV) (Ref. 49), taking the strong dispersion towards the high-energy side, as shown in Ref. 50, into account. The thickness of the depletion layer was determined from a separate measurement of the $I(L_-)/I(\mathrm{LO})$ phonon intensity ratio[30] in the $\bar{z}(y,x)z$ configuration (IV) performed on a conventional double monochromator with an 1800-line/mm grating.

Figure 1 shows the $I(L_-)/I(\mathrm{LO})$ ratio plotted against laser photon energy for the discrete lines of an Ar^+ and Kr^+ laser (the inset depicts a typical spectrum at $\hbar\omega_L=2.336$ eV). The curves are calculated for different

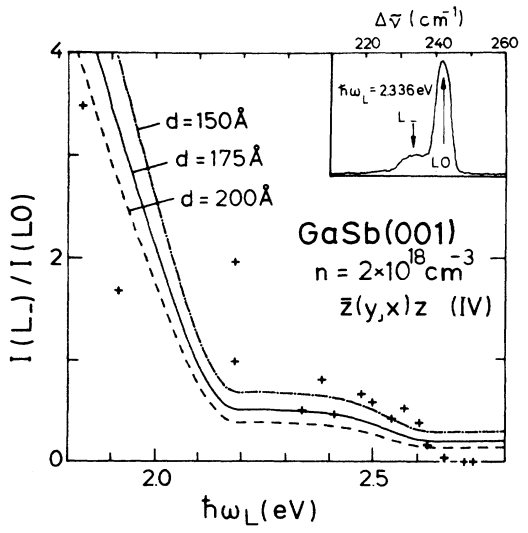

FIG. 1. Ratio of the scattering intensity for screened LO phonons L_- to that for bare LO phonons. The curves are calculated for three depletion layer thicknesses d as described in the text. The inset shows a typical spectrum at $\hbar\omega_L=2.336$ eV.

thicknesses of the depletion layer using the ellipsometric absorption data and assuming that the LO signal is confined to the depletion layer only, while the L_- mode originates from the bulk. For an idealized abrupt change from the depletion region to the doped bulk, $I(L_-)/I(\mathrm{LO})$ is proportional to

$$e^{-(\alpha_L+\alpha_S)d}/(1-e^{-(\alpha_L+\alpha_S)d}) ,$$

where α_L (α_S) is the absorption coefficient at the frequency of the incident (scattered) light and d the thickness of the depletion layer. Although this idealization is rough, the calculated curves for $d=175\pm25$ Å represent the ratio found experimentally rather well. With a simple Schottky model we determine the electric field at the surface to be $|\mathbf{E}|_{max}\cong4\times10^5$ V/cm. The potential barrier then amounts to about 0.4 eV. We thus expect a forbidden contribution to the Raman scattering by LO phonons from the surface depletion layer induced by the built-in electric field.[32,33]

The count rate *outside* the crystal R_S' is related to the Raman scattering efficiency $dS/d\Omega$ by the following expressions.[2,30] For the signal coming from the depletion layer,

$$R_S'=\left[\frac{T_S T_L}{n_S^2(\alpha_L+\alpha_S)}(1-e^{-(\alpha_L+\alpha_S)d})\right]\frac{P_L'}{\hbar\omega_L}\Delta\Omega'\frac{dS}{d\Omega} . \tag{3}$$

For the signal coming from the bulk,

$$R_S'=\left[\frac{T_S T_L}{n_S^2(\alpha_L+\alpha_S)}(e^{-(\alpha_L+\alpha_S)d})\right]\frac{P_L'}{\hbar\omega_L}\Delta\Omega'\frac{dS}{d\Omega} . \tag{4}$$

Here, T_L (T_S) is the power-transmission coefficient ($T=1-r$), n_L (n_S) the refractive index, and α_L (α_S) the absorption coefficient at the frequency ω_L (ω_S) of the incident (scattered) light. Further, d, P_L', and $\Delta\Omega'$ denote the thickness of the depletion layer, the power of the incident light, and the solid angle of collection *outside* the crystal, respectively. The factors in the large parentheses of Eqs. (3) and (4) correct the signals for absorption, refractive index, and reflectivity. The absorption data for Si were taken from Ref. 51, and the reflectivity and refractive index were chosen from ellipsometric data. For the correction of the Si data, Eq. (3) for $d\rightarrow\infty$ was applied.

III. THEORY

The theory of resonant Raman scattering by LO phonons near the E_1 and $E_1+\Delta_1$ gaps has been reviewed in Refs. 8 and 31 for deformation-potential (DP), Fröhlich intraband (F), and electric-field (E)-induced scattering. An additional contribution to the scattering near resonance at the $E_0+\Delta_0$ gap arises from elastic scattering by impurities.[2-8,27] The electric field at the depletion layer may lead to an important "forbidden" contribution to the signal near the E_1 and $E_1+\Delta_1$ gaps. In the bulk the impurities are screened by the electron plasma and thus impurity-induced scattering can be neglected for plasmons. Charge-density fluctuations[12-14] are also dis-

carded near E_1 and $E_1+\Delta_1$ of GaSb, because the amount of free carriers occupying the conduction-band minimum of this gap is very small. Since no ionic deformation is present for plasmons, only those mechanisms associated with their electrical field are operative. Electro-optic (EO) scattering arises from Fröhlich *inter*band coupling with a higher conduction band and obeys usual dipole-selection rules,[12,22,25] whereas Fröhlich *intra*band (F) coupling yields the usual **q**-dependent Raman scattering[26] which is dipole forbidden over a (001) face near the E_1 and $E_1+\Delta_1$ gaps.[8,31]

We apply a formalism similar to that of Ref. 31 to calculate the transition amplitudes and matrix elements for the EO scattering by plasmons, as well as the impurity-induced scattering by LO phonons and the 2LO-phonon scattering. We also rediscuss the formula for F and E scattering of Refs. 31 and 8 as far as prefactors and signs of Raman polarizabilities for LO phonons or plasmons are concerned.

Raman scattering intensities can either be expressed as Raman scattering efficiencies or squared Raman polarizability, which, in the case of first-order Raman scattering by LO phonons, are related to each other by Eq. (1) of Ref. 5. The Raman scattering efficiency $dS/d\Omega$ (per unit solid angle and unit length) depends on the transition amplitude W_{fi} between an initial $|i,\hat{\mathbf{e}}_L\rangle$ and a final state $|f,\hat{\mathbf{e}}_S\rangle$ ($\hat{\mathbf{e}}_L$ and $\hat{\mathbf{e}}_S$ are the polarization vectors for the incident and scattered light):

$$\frac{dS}{d\Omega}=\frac{\omega_S^3\omega_L}{(2\pi)^2}\frac{n_S^3 n_L}{c^4}V\left[\frac{1}{\hbar\omega_L}\right]^2|W_{fi}(\hat{\mathbf{e}}_S,\hat{\mathbf{e}}_L)|^2[n(\Omega)+1]. \tag{5}$$

V is the crystal volume, c the speed of light in vacuum, n_L (n_S) the refractive index at the frequency ω_L (ω_S) of the incident (scattered) light, and $n(\Omega)$ the boson occupation number of an elementary excitation with frequency Ω. In the case of impurity-induced and 2LO-phonon scattering, fourth-order perturbation expressions hold for $W_{fi}(\hat{\mathbf{e}}_S,\hat{\mathbf{e}}_L)$ involving **q** integrations over the LO-phonon branch.[2,34,36] A fourth-order perturbation expression has also been evaluated in Ref. 31 for **E**-induced Raman scattering. In the case of F, EO, and DP scattering by LO phonons or plasmons, a third-order perturbation expression [similar to Eq. (11) of Ref. 31] holds for the transition amplitude.[8,31]

The Raman polarizability a for first-order Raman scattering is related, for either LO phonons or plasmons, to the transition amplitude[2]

$$a=\frac{n_S n_L}{2\pi}\frac{V_c}{\bar{u}_0}\frac{1}{\hbar\omega_L}W_{fi}(\hat{\mathbf{e}}_S,\hat{\mathbf{e}}_L)\ . \tag{6}$$

V_c ($=a_0^3/4$) is the volume of the primitive cell and $\bar{u}_0$ the zero-point amplitude of the relative displacement of the longitudinal elementary excitation (LO phonon or plasmon). This amplitude $\bar{u}_0$ can be derived from the zero-point energy conservation[52]

$$\bar{u}_{0,P}=\left[\frac{\hbar}{2nVm_e\Omega_P}\right]^{1/2}\quad\text{for plasmons} \tag{7}$$

and

$$\bar{u}_{0,\mathrm{LO}}=\left[\frac{\hbar V_c}{2VM^*\Omega_{\mathrm{LO}}}\right]^{1/2}\quad\text{for LO phonons}\ . \tag{8}$$

m_e is the effective electron mass, n the electron concentration, and Ω_P the plasma frequency, whereas M^* [$=(1/M_{\mathrm{Ga}}^{-1}+1/M_{\mathrm{As}}^{-1})^{-1}$] denotes the reduced mass of the primitive cell. Note that the $\bar{u}_0$'s introduce, in Eq. (6), a scaling factor $\bar{u}^2_{0,\mathrm{LO}}/\bar{u}^2_{0,P}=1.4\times10^{-10}$ between the squared Raman polarizability of plasmons with respect to that of LO phonons in GaSb.

Equations (7) and (8) allow us to write the Fröhlich interaction operator H_{F} in a unique form for plasmons and LO phonons:[52]

$$H_{\mathrm{F}}=i\frac{\mathbf{q}\cdot\hat{\mathbf{e}}}{q^2}\frac{C_{\mathrm{F}}}{\sqrt{V}}(c_{\mathbf{q}}^{\dagger}e^{-i\mathbf{q}\cdot\mathbf{r}}-c_{\mathbf{q}}e^{i\mathbf{q}\cdot\mathbf{r}})\ , \tag{9}$$

where $c_{\mathbf{q}}^{\dagger}$ and $c_{\mathbf{q}}$ are the corresponding creation and annihilation operators and $\hat{\mathbf{e}}$ is the phonon (plasmon) polarization vector. Depending on the relative sign of $\hat{\mathbf{e}}$ and C_{F} an additional minus sign appears in Eq. (9) which is essential for the interference phenomenon to be discussed here. For LO-phonon scattering we define $\hat{\mathbf{e}}_{\mathrm{LO}}$ following Ref. 2 (Fig. 1 of Ref. 2, $\mathbf{u}_{\mathrm{rel,LO}}=\mathbf{u}_{\mathrm{anion}}-\mathbf{u}_{\mathrm{cation}}$): $\hat{\mathbf{e}}_{\mathrm{LO}}$ points into the direction of the relative sublattice displacement. We take $\hat{\mathbf{e}}_{\mathrm{LO}}=(0,0,1)$ for propagation along $\hat{\mathbf{z}}$. With this definition the Fröhlich constant becomes

$$\begin{aligned}C_{\mathrm{F,LO}}&=e[2\pi(1/\epsilon_\infty-1/\epsilon_0)\hbar\Omega_{\mathrm{LO}}]^{1/2}\\&=\frac{e_T e}{\epsilon_\infty}\left[\frac{8\pi^2\hbar}{V_c M^*\Omega_{\mathrm{LO}}}\right]^{1/2}>0\ .\end{aligned} \tag{10}$$

ϵ_∞ and ϵ_0 are the high-frequency (ir) and low-frequency (rf) dielectric constants. Equation (10) defines the transverse dynamical charge e_T, which is positive within our definition of the primitive cell. An interchange of the cation and anion would change the sign of e_T, and thus that of C_{F}, if $\hat{\mathbf{e}}_{\mathrm{LO}}$ is kept constant.

By analogy we define in the case of the plasmon ($\mathbf{u}_{\mathrm{rel},P}=\mathbf{u}_{\mathrm{electron}}$): $\hat{\mathbf{e}}_P$ points into the direction of the electron displacement [$\hat{\mathbf{e}}_P=(0,0,1)$ for propagation along $\hat{\mathbf{z}}$], and

$$C_{\mathrm{F},P}=e\left[\frac{2\pi\hbar\Omega_P}{\epsilon_\infty}\right]^{1/2}>0\ . \tag{11}$$

The choice of the sign in Eq. (11) is consistent with that of Eq. (10). Note that the sign of C_{F} for plasmons does not depend on the choice of the origin in the primitive cell (PC).

A. Scattering mechanisms

The electron-photon interaction H_{eR} enters twice into the third- or fourth-order expressions for the transition amplitude [Eq. (11) of Ref. 31]. It yields the matrix element

$$\langle 0 \mid b^{cv}_{\mathbf{k}'\mathbf{k}} H_{eR} a^{\dagger}_{\mathbf{k}_i\hat{\mathbf{e}}_i} \mid 0\rangle = \frac{e}{m}\left[\frac{4\pi}{V n_i^2}\right]^{1/2}\left[\frac{\hbar}{2\omega_i}\right]^{1/2} \times \langle c \mid \hat{\mathbf{e}}_i\cdot\mathbf{p} \mid v\rangle \delta_{\mathbf{k}_i,\mathbf{k}'} , \quad (12)$$

where e (m) is the free-electron charge (mass), n_i is the refractive index of the material at the frequency ω_i, and $\langle c \mid \hat{\mathbf{e}}_i\cdot\mathbf{p} \mid v\rangle$ denotes the momentum matrix element between a valence-band state and a conduction-band state for a polarization $\hat{\mathbf{e}}_i$ of $\mathbf{p}$. $a^{\dagger}_{\mathbf{k}\hat{\mathbf{e}}}$ and $b^{\dagger cv}_{\mathbf{k}\mathbf{k}}$ are creation operators for a photon with momentum $\hbar\mathbf{k}$ and a polarization $\hat{\mathbf{e}}$, and an electron-hole (e-h) pair with total pseudomomentum $\hbar\mathbf{k}$ ($\mathbf{k}=\mathbf{k}_e-\mathbf{k}_h$) and relative pseudomomentum $\hbar\mathbf{K}$ ($\mathbf{K}=s_e\mathbf{k}_e+s_h\mathbf{k}_h$), respectively. The dimensionless quantities $s_{e,h}$ are defined as

$$s_e=m_{e\perp}/m_\perp, \quad s_h=m_{h\perp}/m_\perp, \quad m_\perp=m_{e\perp}+m_{h\perp} . \quad (13)$$

$m_{e\perp}$ ($m_{h\perp}$) are the conduction-electron (-hole) effective masses in the direction perpendicular to [111], respectively. In order to evaluate the resonance behavior near the E_1 gap, the transition amplitudes W_{fi} must be summed over all eight valleys along the $\langle 111\rangle$ directions [Eqs. (18) and (19) of Ref. 31].

1. *Electro-optic (EO) scattering by plasmons or LO phonons*

The Raman polarizability for EO scattering by plasmons (LO phonons) can be calculated in third-order perturbation theory. In Eq. (11) of Ref. 31 the *interband* matrix element has to replace the *intraband* matrix element of the Fröhlich interaction. Three bands are involved instead of two. We use a three-band model consisting only of the $\Lambda^v_{4,5}$ (Λ^v_6) valence band for excitations resonant with the E_1 ($E_1+\Delta_1$) gap, the $\Lambda^{c,l}_6$ lowest conduction band and the $\Lambda^{c,u}_6\oplus\Lambda^c_{4,5}$ higher conduction bands. The energies of e-h transitions are labelled[24] E_1 ($\Lambda^v_{4,5}\rightarrow\Lambda^{c,l}_6$), $E_1+\Delta_1$ ($\Lambda^v_6\rightarrow\Lambda^{c,l}_6$), and $\bar{E}'_1$ ($\Lambda^v_{4,5}$ or $\Lambda^v_6\rightarrow\Lambda^{c,u}_6$ or $\Lambda^c_{4,5}$). The spin-orbit splitting and the dispersion are neglected for the higher E'_1 transition. Its average energy is denoted by $\bar{E}'_1$. For the E_1 gap a parabolic dispersion is assumed:[31]

$$E_1(\mathbf{K})=E_1+\frac{\hbar^2}{2\mu_\perp}K_\perp^2-i\eta^+ . \quad (14)$$

$\mu_\perp$ [$=(1/m_{e\perp}+1/m_{h\perp})^{-1}$] denotes the reduced mass of an e-h pair in the direction perpendicular to the [111] direction, and η^+ is the Lorentzian broadening of the E_1 gap. We consider free-electron-hole pairs only.

The electric field associated with the plasmon (LO phonon) couples two different bands [vector potential $\mathbf{A}=i(c^2/V)^{1/2}(C_F/e\Omega)(c^{\dagger}_{\mathbf{q}}e^{-i\mathbf{q}\cdot\mathbf{r}}-c_{\mathbf{q}}e^{i\mathbf{q}\cdot\mathbf{r}})\hat{\mathbf{e}}$]. The *interband* matrix element of the Fröhlich interaction is

$$\langle 0 \mid b^{c'v}_{\mathbf{k}'\mathbf{k}} c_{\mathbf{q}} H_F^{\text{inter}} b^{\dagger cv}_{\mathbf{k}\mathbf{k}} \mid 0\rangle = i\left[\frac{e}{m}\right]\left[\frac{1}{V}\right]^{1/2}\frac{C_F}{e\Omega}\langle c' \mid \hat{\mathbf{e}}\cdot\mathbf{p} \mid c\rangle \delta_{\mathbf{K},\mathbf{K}'}\delta_{\mathbf{k},\mathbf{k}'+\mathbf{q}} . \quad (15)$$

The matrix element of Eq. (15) describes the scattering of an electron from one band (c) to the other (c') while an elementary excitation is created with pseudomomentum $\hbar\mathbf{q}$.

The momentum matrix elements $\langle c' \mid \hat{\mathbf{e}}\cdot\mathbf{p} \mid c\rangle$ or $\langle c \mid \hat{\mathbf{e}}\cdot\mathbf{p} \mid v\rangle$ of Eqs. (12) and (15) between the three bands Λ^v_6 or $\Lambda^v_{4,5}$, $\Lambda^{c,l}_6$, and $\Lambda^{c,u}_6$ or $\Lambda^c_{4,5}$ are defined as follows:[45,53]

$$P=i\langle X_v \mid p_x \mid S\rangle \geqq 0 \quad (\Lambda^{c,l}_6\rightarrow\Lambda^v_6 \text{ or } \Lambda^v_{4,5}) , \quad (16a)$$

$$P'=i\langle S \mid p_x \mid X_c\rangle \leqq 0 \quad (\Lambda^{c,u}_6 \text{ or } \Lambda^c_{4,5}\rightarrow\Lambda^{c,l}_6) , \quad (16b)$$

and

$$Q=i\langle X_v \mid p_y \mid Z_c\rangle \geqq 0 \quad (\Lambda^{c,u}_6 \text{ or } \Lambda^c_{4,5}\rightarrow\Lambda^v_6 \text{ or } \Lambda^v_{4,5}) . \quad (16c)$$

This definition implies that the matrix elements do not vary much from the Γ to the L point along the Λ direction.[54] P, P', and Q are real numbers. The sign of P' (but not that of P and Q) reverses when we interchange cation and anion within the PC. In Eqs. (16), X_v, Y_v, and Z_v (X_c, Y_c, and Z_c) denote the valence- (conduction-) band functions that transform like the coordinates x, y, and z, respectively.

The summation of the transition amplitudes in Eqs. (18) and (19) of Ref. 31 leads to a factor of 2 to take into account opposite $\langle 111\rangle$ directions. All possible intermediate states ($\mid c\rangle = \mid \Lambda^{c,l}_6\rangle$, $\mid \Lambda^{c,u}_6\rangle$, or $\mid \Lambda^c_{4,5}\rangle$) and the spin degeneracy must be included. For backscattering on a (001) face, the product of momentum matrix elements in the numerator of the transition amplitude averaged over the four different valleys ($l=1$, [111]; $l=2$, [$1\,\bar{1}\,\bar{1}$]; $l=3$, [$\bar{1}1\bar{1}$]; $l=4$, [$\bar{1}\bar{1}1$]) becomes

$$\sum_{l=1}^{4}\langle v \mid \hat{\mathbf{e}}_S\cdot\mathbf{p} \mid c'\rangle_l\langle c \mid \hat{\mathbf{e}}_L\cdot\mathbf{p} \mid v\rangle_l\langle c' \mid p_z \mid c\rangle_l = \frac{20iPP'Q}{9}\hat{\mathbf{e}}_S\cdot\overleftrightarrow{\mathbf{T}}_z\cdot\hat{\mathbf{e}}_L , \quad (17)$$

with

$$\overleftrightarrow{\mathbf{T}}_z=\begin{bmatrix}0&1&0\\1&0&0\\0&0&0\end{bmatrix} .$$

The denominator of the transition amplitude determines the resonance behavior of the contributing diagrams. We can distinguish between two resonant terms which contribute to the transition amplitude with opposite signs depending on whether they correspond to *incoming* or *outgoing* resonances ($\hbar\omega_L$ or $\hbar\omega_S=E_1$). It is convenient to introduce the quantities[31]

$$a^*=(\hbar/2\mu_\perp\Omega)^{1/2}, \quad \alpha=\frac{\hbar\omega_L-E_1+i\eta^+}{\hbar\Omega}$$

and (18)

$$\beta=\alpha-1 .$$

The longitudinal $\mathbf{K}$ integration yields $f\pi\sqrt{3}/a_0$ with

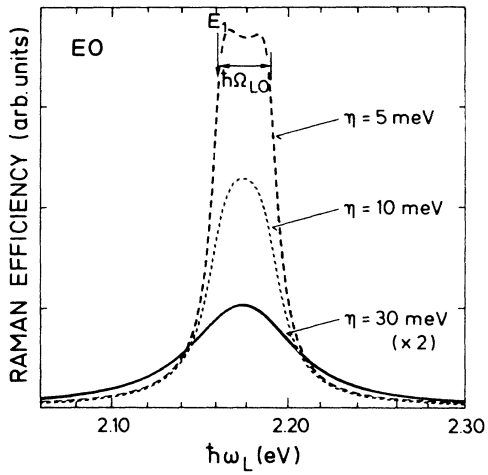

FIG. 2. Raman efficiency for electro-optic (EO) scattering calculated with Eq. (19) using the parameters appropriate to the LO phonon of GaSb for three different broadenings of the E_1 gap ($\eta=5$, 10, and 30 meV).

$f\approx\frac{3}{4}$ for III-V compounds.[31,55] The final result for the EO Raman tensor $\overleftrightarrow{R}_{EO,z}$ near E_1 ($E_1+\Delta_1$) is then given by (**q** along z)

$$\overleftrightarrow{R}_{EO,z}=a_{EO}\overleftrightarrow{T}_z ,$$

where

$$a_{EO}=\frac{5\sqrt{3}f}{9\pi a_0 a^{*2}}\frac{1}{\omega_L(\omega_L\omega_S)^{1/2}}\left[\frac{e}{m}\right]^3\frac{V_c}{V^{1/2}\bar{u}_0}PP'Q\frac{C_F}{e\Omega}\times\left[\frac{1}{\bar{E}'_1}+\frac{1}{\bar{E}'_1-\hbar\omega_L}\right](\ln\beta-\ln\alpha) . \quad (19)$$

The EO Raman scattering obeys usual dipole-selection rules. On a (001) face it is allowed for $\hat{e}_L=(1,0,0)$ and $\hat{e}_S=(0,1,0)$.

Figure 2 displays the Raman scattering efficiency for EO scattering as a function of laser energy $\hbar\omega_L$ near the E_1 gap. The calculation was performed for different broadenings η with parameters appropriate to LO phonons in GaSb. Incoming and outgoing resonances are observed: for $\eta=0$ the scattering efficiency diverges at $\hbar\omega_L=E_1$ and $\hbar\omega_S=E_1$. With increasing broadening the curves smear out and show a maximum at $\hbar\omega_L=E_1+\hbar\Omega_{LO}/2$. The sign of a_{EO} depends on the sign of the product of $PP'Q$ (<0, with our choice of PC). It reverses for an interchange of cations and anions within the PC. However, it does not change sign in going from the resonance near E_1 to that near $E_1+\Delta_1$: The EO scattering is a process which involves a third *higher* band.

2. q-dependent (F) scattering by plasmons or LO phonons

The Raman polarizability a_F for **q**-induced Raman scattering has been evaluated, in Ref. 31, in third-order perturbation theory [Eqs. (11)–(23) of Ref. 31]. The derivation is formally similar to that of the EO scattering. A two-band model consisting either of the $\Lambda^v_{4,5}$ valence and $\Lambda^{c,l}_6$ conduction band (E_1) or the Λ^v_6 and $\Lambda^{c,l}_6$ band ($E_1+\Delta_1$) is considered and the Fröhlich *intraband* matrix element included[31,52]

$$\langle 0\,|\,b_{k'K'}c_q H_F^{intra}b^\dagger_{kK}\,|\,0\rangle = \frac{i\hat{e}\cdot\mathbf{q}}{q^2}\frac{C_F}{\sqrt{V}}(\delta_{K,s_e q+K'}-\delta_{K+s_h q,K'})\delta_{k,k'+q} , \quad (20)$$

where the dimensionless quantities s_e, s_h are defined in Eq. (13). We consider only free electron-hole pairs and take the **q** dependence into account by expanding the denominator to second order in **q**. The final result for the Raman tensor $\overleftrightarrow{R}_F$ after summing over all valleys and the spin degeneracy can be summarized as[31,37]

$$\overleftrightarrow{R}_F=-i\frac{\sqrt{3}f}{4\pi a_0}\frac{1}{\omega_L(\omega_L\omega_S)^{1/2}}\left[\frac{e}{m}\right]^2\frac{V_c}{V^{1/2}\bar{u}_0}P^2\frac{C_F}{(\hbar\Omega)^2}\times(s_e-s_h)\hat{e}\cdot\mathbf{q}\left[\frac{\partial}{\partial\beta}+\beta\frac{\partial^2}{\partial\beta^2}\right]\frac{\ln\beta-\ln\alpha}{\alpha-\beta}\times\sum_{l=1}^{4}\frac{2}{q^2}(\mathbf{q}\cdot\overleftrightarrow{T}_l\cdot\mathbf{q})\overleftrightarrow{T}_l . \quad (21)$$

The vectors $\hat{e}_l$ are unit vectors pointing in the direction of the lth valley. The $\overleftrightarrow{T}_l$ ($l=1,2,3,4$) matrices are defined as[37]

$$\overleftrightarrow{T}_1=\frac{1}{6}\begin{bmatrix}2&-1&-1\\-1&2&-1\\-1&-1&2\end{bmatrix},\quad \overleftrightarrow{T}_2=\frac{1}{6}\begin{bmatrix}2&1&1\\1&2&-1\\1&-1&2\end{bmatrix},$$
$$\overleftrightarrow{T}_3=\frac{1}{6}\begin{bmatrix}2&1&-1\\1&2&1\\-1&1&2\end{bmatrix},\quad \overleftrightarrow{T}_4=\frac{1}{6}\begin{bmatrix}2&-1&1\\-1&2&1\\1&1&2\end{bmatrix} . \quad (22)$$

In general, $\overleftrightarrow{R}_F$ is a *non*diagonal tensor. For backscattering on a (001) face it becomes diagonal, since $(2/q^2)(\mathbf{q}\cdot\overleftrightarrow{T}_l\cdot\mathbf{q})=\frac{2}{3}$ ($l=1,2,3,4$) and $\sum_{l=1}^4\overleftrightarrow{T}_l=\frac{4}{3}\overleftrightarrow{1}$. With

$$\left[\frac{\partial}{\partial\beta}+\beta\frac{\partial^2}{\partial\beta^2}\right]\frac{(\ln\beta-\ln\alpha)}{(\alpha-\beta)}=2+(\alpha+\beta)(\ln\beta-\ln\alpha) ,$$

Eq. (21) simplifies to ($\overleftrightarrow{R}_F=a_F\overleftrightarrow{1}$) (Refs. 8 and 31),

$$a_F=i\frac{2\sqrt{3}}{9\pi}\frac{f}{a_0}\frac{1}{\omega_L(\omega_L\omega_S)^{1/2}}\left[\frac{e}{m}\right]^2\frac{V_c}{V^{1/2}\bar{u}_0}P^2\frac{C_F}{(\hbar\Omega)^2}\times(s_e-s_h)q[2+(\alpha+\beta)(\ln\beta-\ln\alpha)] . \quad (23)$$

For Raman scattering by LO phonons, Eq. (23) differs from Eq. (8) of Ref. 8 by a factor a^*/a_0, and $\frac{2}{3}$, which were inadvertently omitted.

A comparison of Eq. (23) with (19) shows that the susceptibility of Fröhlich *intraband* **q**-dependent scattering is proportional to the frequency derivatives of the function $\ln\beta-\ln\alpha$ (two-band process), whereas the *inter*band EO scattering is simply proportional to $\ln\beta-\ln\alpha$ (three-band process).

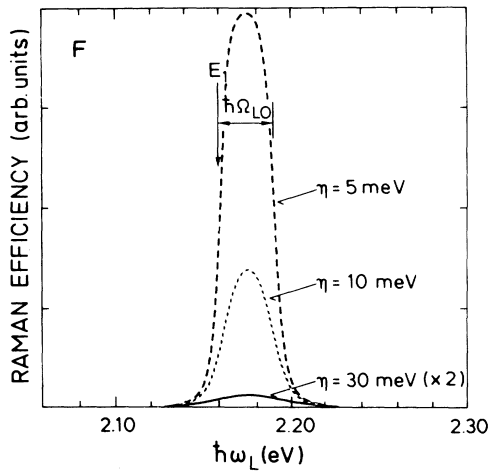

FIG. 3. Raman efficiency for q-induced forbidden (F) scattering calculated with Eq. (23) using the parameters appropriate to the LO phonon of GaSb for three different broadenings of the E_1 gap ($\eta=5$, 10, and 30 meV).

Figure 3 shows the results of calculations with Eq. (23), using the same parameters as in Fig. 2. It reveals the sharper resonance and the stronger enhancement of the F-induced scattering as compared with Fig. 2. There are also single resonances at $\hbar\omega_L=E_1$ (incoming) and $\hbar\omega_S=E_1$ (outgoing). Both divergences are removed by the finite broadening η of the gap. Already for $\eta=5$ meV, the resonance maximum occurs at $E_1+\hbar\Omega_{LO}/2$ (compare with the dashed curve of Fig. 2). The F scattering is more affected by the broadening of the E_1 gap than the EO scattering. The sign of a_F depends only on the difference in the masses $m_{e\perp}-m_{h\perp}$ (<0), and on C_F. It is the same for LO phonons and plasmons for our definition of the PC and remains the same at the E_1 and $E_1+\Delta_1$ gaps. For opposite faces a_F changes sign, while a_{EO} does not.

3. *Surface-field-induced (E) scattering by LO phonons*

The effect of an external or built-in (depletion layer) electric field consists of two parts. The purely electronic contribution (Franz-Keldysh mechanism)[56] corresponds to the separation of electron and hole in the intermediate states induced by the electric field.[33] The second contribution arises from the relative sublattice displacements induced by the field and a resulting modification of the phonon properties.[57]

Whereas the second mechanism is important in paraelectric crystals with "soft-mode" behavior,[58] the Franz-Keldysh mechanism has been shown to be important in III-V semiconductors.[32] The electric field leads to an enhancement of the dipole-forbidden Raman scattering [electric-field-induced Raman scattering (EFIRS)]. It has been used to investigate the electric field in space-charge regions at surfaces and interfaces.[30,32,33,59,60] For excitation close to the E_1 and $E_1+\Delta_1$ gaps of III-V compounds, when the light penetration factor $\frac{1}{2}\alpha$ (100–200 Å in GaSb) is of the order of the thickness of the depletion layer (175 Å in our sample), the electric-field-induced Raman scattering by LO phonons cannot be neglected (electric fields of the order of 10^5 V/cm are obtained near the surface).[32,59]

The resonance of the two-band scattering processes by LO phonons near the E_1 gap via the Franz-Keldysh mechanism has been calculated by several authors in fourth-order perturbation theory.[31,33,61] It involves the Fröhlich intraband coupling and the matrix element of the interaction H_E between the electron-hole pair and the electric field:

$$\langle 0 \mid b_{\mathbf{k}'\mathbf{K}'} H_E b^{\dagger}_{\mathbf{k}\mathbf{K}} \mid 0 \rangle = -i\delta_{\mathbf{k},\mathbf{k}'} e(\mathbf{E}\cdot\nabla_{\mathbf{K}})\delta_{\mathbf{K},\mathbf{K}'} . \quad (24)$$

Equation (24) is valid as long as the characteristic electro-optic energy is small when compared with the damping of the electron states.[62] The final expression for the E-induced Raman tensor corresponding to LO phonons is similar to that of q-dependent F-induced scattering:[31]

$$\overleftrightarrow{R}_E = -\frac{\sqrt{3}f}{4\pi a_0}\frac{1}{\omega_L(\omega_L\omega_S)^{1/2}}\left[\frac{e}{m}\right]^2\frac{V_c}{V^{1/2}\bar{u}_{0,LO}}P^2\frac{eC_{F,LO}}{(\hbar\Omega_{LO})^3} \times \hat{\mathbf{e}}_{LO}\cdot\mathbf{E}\left[\frac{\partial}{\partial\alpha}+\frac{\partial}{\partial\beta}\right]\left[\frac{\partial}{\partial\beta}+\beta\frac{\partial^2}{\partial\beta^2}\right]\frac{\ln\beta-\ln\alpha}{\alpha-\beta} \times \sum_{l=1}^{4}\frac{2}{Eq}(\mathbf{E}\cdot\overleftrightarrow{T}_l\cdot\mathbf{q})\overleftrightarrow{T}_l . \quad (25)$$

In general, $\overleftrightarrow{R}_E$ (like $\overleftrightarrow{R}_F$) is a *non*diagonal tensor. For backscattering at a (001) face with $\mathbf{E}/\mid\mathbf{E}\mid=(0,0,\bar{1})$ it becomes diagonal, since $(2/Eq)\mathbf{E}\cdot\overleftrightarrow{T}_l\cdot\mathbf{q}=-\frac{2}{3}$ ($l=1,2,3,4$) and $\sum_{l=1}^{4}\overleftrightarrow{T}_l=\frac{4}{3}\overleftrightarrow{1}$. Carrying out the frequency derivatives simplifies to ($\overleftrightarrow{R}_E=a_E\overleftrightarrow{1}$) (Refs. 8, 31, and 61):

$$a_E = -\frac{2\sqrt{3}}{9\pi}\frac{f}{a_0}\frac{1}{\omega_L(\omega_L\omega_S)^{1/2}}\left[\frac{e}{m}\right]^2\frac{V_c}{V^{1/2}\bar{u}_{0,LO}}P^2 \times\frac{eC_{F,LO}}{(\hbar\Omega_{LO})^3}\mid\mathbf{E}\mid\left[2(\ln\beta-\ln\alpha)+\frac{1}{\alpha}+\frac{1}{\beta}\right] . \quad (26)$$

Figure 4(a) (upper part) compares the result of calculations with Eq. (26) (using the parameters appropriate to the LO phonon of GaSb and $\eta=30$ meV) with that of Eq. (23) for F-induced dipole-forbidden scattering. The resonance line shape for E-induced scattering is very similar, however, it leads to a sharper resonance, as expected from the fact that it depends on higher-order derivatives. The ratio of the E-scattering with respect to the F-scattering efficiency can be estimated for large broadenings, as in the case of the E_1 gap, to be at the resonance maxima $\mid eE/i\eta\mid^2/\mid i(s_e-s_h)q\mid^2$. It equals about 50 for the E_1 gap of GaSb (assuming $E=10^5$ V/cm).[32]

We also see from Fig. 4(b) (lower part) that the real and imaginary parts of a_E and a_F are also quite similar in magnitude and sign, with the a_E curves somewhat sharper than the a_F counterparts.

One additional complication arises for the surface-

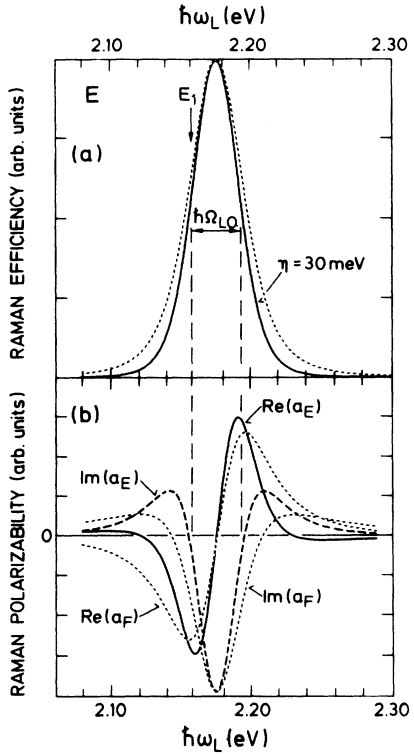

FIG. 4. (a) Raman efficiency for **E**-induced forbidden (E) scattering calculated with Eq. (26) using the parameters appropriate to the LO phonon of GaSb for $\eta=30$ meV (solid line). The dotted line represents the results of a calculation with Eq. (23) and identical parameters for **q**-dependent forbidden (F) scattering. (b) Comparison of the real and imaginary parts of a_E with the corresponding ones of a_F (dotted curves).

field-induced scattering. The electric field decreases, within a simple Schottky model, linearly from the surface to the end of the depletion layer.[32,59,60] The EFIRS signal of the LO-phonon scattering is therefore given by a weighted average over the distance from the surface $I_{LO}\sim\int_0^d E^2(z)e^{-z2\alpha}dz$. Hence, the best way to separate the **q**-dependent dipole-forbidden Raman scattering and the EFIRS would be the application of an external electric field which produces flat-band conditions.[13,32,59]

In order to investigate the interference effects of bare LO phonons near the E_1 and $E_1+\Delta_1$ gaps (arising in the depletion layer), we assume that the forbidden scattering is of the Fröhlich type. The field-induced effect can be approximately taken into account, in view of the discussion above, by simply increasing the prefactor of the expressions for a_F.

4. *Deformation-potential (DP) scattering by LO phonons*

The deformation-potential scattering by LO phonons obeys the usual dipole-selection rules. For backscattering at a (001) face its Raman tensor has the form

$$\overleftrightarrow{R}_{DP,z}=a_{DP}\overleftrightarrow{T}_z\ , \tag{27}$$

where $\overleftrightarrow{T}_z$ is defined in Eq. (17) and a_{DP} is the corresponding Raman polarizability. The EO scattering is thus isomorphic to the DP scattering. The EO scattering gives rise to the difference between Raman scattering by LO phonons (to which it contributes) with respect to TO phonons (it does not contribute). The ratio between the Raman polarizability a_{LO} and a_{TO} is used to define the Faust-Henry coefficient C;[22,63]

$$\frac{a_{LO}}{a_{TO}}=1-\frac{\Omega_{LO}^2-\Omega_{TO}^2}{C\Omega_{TO}^2}\ . \tag{28}$$

Usually, the EO contribution to the LO-phonon scattering is small.[38] We therefore assume, for $a_{LO}\cong a_{DP}$, i.e., the following dependence on energy near the E_1 and $E_1+\Delta_1$ gaps:[8,22]

$$a_{DP}=\frac{a_0^2}{4\sqrt{6}}\left[-\frac{1}{2\sqrt{2}}d_{1,0}^5\times\left[\frac{d\chi^+(E)}{dE}\bigg|_{E_1}+\frac{d\chi^-(E)}{dE}\bigg|_{E_1+\Delta_1}\right]+2d_{3,0}^5\frac{\chi^+(E)-\chi^-(E)}{\Delta_1}+B\right]\ . \tag{29}$$

Equation (29) describes a_{DP} as a function of a strongly resonant two-band contribution (deformation potential $d_{1,0}^5$) and a less resonant three-band term ($d_{3,0}^5$). The constant B accounts for contributions of interband transitions far from the E_1 and $E_1+\Delta_1$ gaps. In Eq. (29), χ^+ and χ^- are the dielectric susceptibilities of the E_1 and $E_1+\Delta_1$ gaps, respectively [Eqs. (1) and (2)]. The derivatives $d\chi^+/dE$ in the two-band terms must be replaced by the finite difference ratios of the susceptibilities at $E=\hbar\omega_L$ and $E=\hbar\omega_S$, if the phonon energies cannot be neglected with respect to $|\hbar\omega_L-E_1+i\eta^+|$ or $|\hbar\omega_L-E_1-\Delta_1+i\eta^-|$. For $\hbar\Omega_{LO}\cong\eta^{\pm}$, the error in using the derivative instead of the finite difference is small ($<10\%$).[8]

The two-band terms produce a sharp resonance maximum near $E_1+\hbar\Omega_{LO}/2$ and $E_1+\Delta_1+\hbar\Omega_{LO}/2$ for $\hbar\Omega_{LO}\lesssim\eta^+,\eta^-$. The sign of their contribution to a_{DP} does not change from E_1 to $E_1+\Delta_1$. The three-band terms cause a broader resonance between E_1 and $E_1+\Delta_1$. The sign of the contribution of the three-band terms to a_{DP} reverses as one goes from E_1 to $E_1+\Delta_1$, since the LO phonons couple the $\Lambda_{4,5}^v$ and Λ_6^v valence bands with each other and the corresponding energy denominator reverses sign. The sign of a_{DP} does not depend on the choice of the cation and anion positions in the PC but only on the sign of the deformation potentials ($d_{1,0}^5<0$, $d_{3,0}^5>0$).[8,64]

5. *Impurity-induced Raman scattering by LO phonons*

A "forbidden" Raman scattering mechanism involving elastic scattering by ionized impurities has been suggested by Gogolin and Rashba.[27] It is a fourth-order process in which the exciton is scattered twice, once by the LO phonon via the Fröhlich *intraband* interaction and

once by the Coulomb potential of an ionized impurity. For the case of the resonance near the $E_0+\Delta_0$ gap, the squared Raman polarizability has been calculated in Ref. 2. It yields a diagonal Raman tensor (dipole-forbidden scattering). The scattering intensity of the higher-order process can dominate over the quadrupole, q-dependent Raman scattering because phonons with much larger wave vector are involved: The impurities carry away the difference between this wave vector and the small optical scattering vector.

The squared Raman polarizability $|\hat{\mathbf{e}}_S\cdot\vec{\mathbf{R}}_{Fi}\cdot\hat{\mathbf{e}}_L|^2=|a_{Fi}|^2$ depends on the transition amplitude $W_{fi}(\hat{\mathbf{e}}_S,\hat{\mathbf{e}}_L,\mathbf{q},\mathbf{q}')$ of impurity-induced scattering by LO phonons (pseudomomentum $\hbar\mathbf{q}$, momentum transfer by the impurity $\hbar\mathbf{q}'$) through

$$|a_{Fi}|^2=\left[\frac{n_S n_L}{2\pi}\right]^2\left[\frac{V_c}{\bar{u}_{0,\mathrm{LO}}}\right]^2\left[\frac{1}{\hbar\omega_L}\right]^2(n_I V)\frac{V}{(2\pi)^3}\times\int\int d\mathbf{q}'\,d\mathbf{q}\,|W_{fi}(\hat{\mathbf{e}}_S,\hat{\mathbf{e}}_L,\mathbf{q},\mathbf{q}')|^2\times\delta(\mathbf{k}_L-\mathbf{k}_S-\mathbf{q}-\mathbf{q}')\,. \tag{30}$$

The form of Eq. (30) is similar to that of Eq. (6); however, the transition probability $|W_{fi}(\hat{\mathbf{e}}_S,\hat{\mathbf{e}}_L)|^2$ is now given by an integral over the $\mathbf{q}$ of the phonon branch weighted by the number of impurities $n_I V$ within the probing volume (n_I denotes the concentration of impurities). The transition amplitude $W_{fi}(\hat{\mathbf{e}}_S,\hat{\mathbf{e}}_L,\mathbf{q},\mathbf{q}')$ can be evaluated from a fourth-order perturbation expression. The most resonant terms include as a first step the annihilation of the incident photon while an e-h pair is created, and as the last step the creation of the scattered photon under recombination of an e-h pair. The two intermediate steps are either scattering first by the phonon and then by the impurity yielding an outgoing double resonance at $\hbar\omega_L=E_1+\hbar\Omega_{\mathrm{LO}}$, or the inverse (incoming double resonance, $\hbar\omega_L=E_1$). The assumptions made for the calculations are mainly the same as for the EO, F, and DP processes. In order to carry out the $\mathbf{q}$ integration in Eq. (30) analytically we have to assume bands independent of $\mathbf{k}$ along the Λ direction (two-dimensional bands, a condition more stringent than two-dimensional critical points). This crude assumption is corrected *a posteriori* in part by introducing a larger broadening η for the corresponding gap. The effect of the neglected slope of the bands in the Λ direction is to carry away (add) kinetic energy to the electrons or holes scattered into intermediate states. It thus reduces the double resonance, since the corresponding denominator in the perturbation expression does not vanish for all $K_\parallel$. An increased broadening η should be able to simulate this effect qualitatively. It must be interpreted as a weighted value of the energy denominator over those $\mathbf{q}$ vectors of LO phonons that contribute mostly to the impurity-induced scattering. Since the LO phonons of interest are close to the center of the Brillouin zone ($q\leqq 0.2/a_0$),[2] the increase in η should be small. We took it to be 10 meV, a value which leads to reasonable agreement between the experimental and calculated two-phonon resonances.

The final result is obtained by summing the transition amplitudes over the different valleys including spin degeneracy, and integrating in cylindrical coordinates over the density of states ($\mathbf{K}$ integration) and over the whole phonon branch assumed to be independent of $\mathbf{q}$. The last integration is expected to overestimate the scattering intensity.

For the calculation, we take the Fourier transform of the screened Coulomb potential to be[2]

$$V_s(\mathbf{q})=\frac{4\pi e^2}{(q_\perp^2+q_\parallel^2+q_F^2)\epsilon_0 V}e^{i\mathbf{q}\cdot\mathbf{r}}\,. \tag{31}$$

Here, $q_\perp$ ($q_\parallel$) is the wave vector parallel (perpendicular) to the [111] direction and ϵ_0 the low-frequency dielectric constant. For our purpose, we shall approximate the screening wave vector q_F by one-half of the distance between impurities [$q_F=2/\lambda=2(4\pi n_I/3)^{1/3}$], an approximation which should represent screening by compensated impurities, but also should not be too bad in the case of screening by ionized impurities. In the bulk, the appropriate wave vector will be given by the Fermi-Thomas screening length. The matrix element of the electron-impurity interaction then becomes

$$\langle 0|b_{\mathbf{k}'\mathbf{K}'}H_{ei}(\mathbf{q})b^\dagger_{\mathbf{k}\mathbf{K}}|0\rangle=\frac{4\pi e^2}{(q^2+q_F^2)\epsilon_0 V}\times(\delta_{\mathbf{K},s_e\mathbf{q}+\mathbf{K}'}-\delta_{\mathbf{K}+s_h\mathbf{q},\mathbf{K}'})\times\delta_{\mathbf{k},\mathbf{k}'+\mathbf{q}}\,. \tag{32}$$

Carrying out all the integrations, the squared Raman polarizability is found to be

$$|a_{Fi}|^2=\frac{16f^2}{3\pi^2}\left[\frac{1}{\omega_L^3\omega_S}\right]\left[\frac{e^2}{m}\right]^4\left[\frac{2M^*\Omega_{\mathrm{LO}}}{\hbar}\right]\times\left[\frac{P^2C_F}{\epsilon_0}\right]^2 n_I V_c\frac{1}{(\hbar\Omega_{\mathrm{LO}})^6 a_0^2 a^{*4}}\times\int_0^\infty q_\perp dq_\perp A(q_\perp)|X(a^*q_\perp)|^2\,. \tag{33}$$

The functions $A(q_\perp)$ and $X(a^*q_\perp)$ are defined in the Appendix. $X(a^*q_\perp)$ results from the integration of the density of states in the direction perpendicular to [111], whereas $A(q_\perp)$ arises from the integration over the phonon branch in the direction parallel to [111]. They both depend on the laser energy $\hbar\omega_L$ through the dimensionless quantities α and β [Eq. (18)]. Figure 5 shows the result of calculations with Eqs. (33), (A2), and (A6) for parameters appropriate to the E_1 gap of GaSb and different effective broadenings η of the E_1 gap. For small broadenings, two distinct peaks are seen which correspond to the double resonances at $\hbar\omega_L=E_1$ (incoming) and $\hbar\omega_L=E_1+\hbar\Omega_{\mathrm{LO}}$ (outgoing), *the outgoing one being dominant.* The divergences found for $\eta=0$ disappear for finite η, and the resonance curves smear out rapidly for increasing η while the peak maxima decrease. At $\eta=40$ meV (as chosen for the E_1 gap of

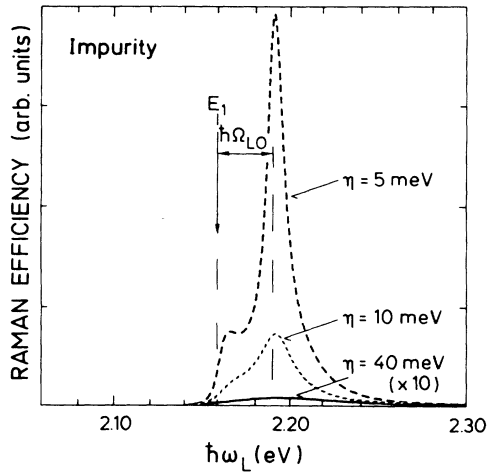

FIG. 5. Raman efficiency for impurity-induced forbidden scattering by one LO phonon calculated with Eqs. (33), (A2), and (A6) using the parameters appropriate to GaSb for three different broadenings of the E_1 gap ($\eta=5$, 10, and 40 meV).

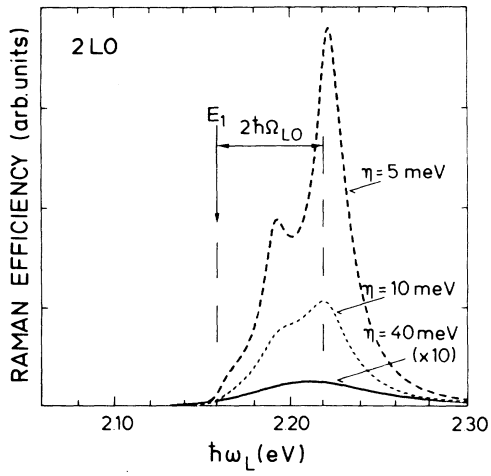

FIG. 6. Raman efficiency for scattering by two LO phonons calculated with Eqs. (34), (A3), and (A7) using the parameters appropriate to GaSb for three different broadenings of the E_1 gap ($\eta=5$, 10, and 40 meV).

GaSb) only one maximum is seen, close to $E_1+\hbar\Omega_{LO}$ (outgoing resonance).

6. *Two-LO-phonon scattering*

The calculation of the scattering by the 2LO phonon near the E_1 and $E_1+\Delta_1$ gaps is formally similar to that of the impurity-induced scattering. One has only to replace the vertex of the electron-impurity interaction by a second Fröhlich intraband interaction [Eq. (20)].[34,36] The terms arising from the permutations of the Fröhlich interactions are identical and yield a factor of 2 for the transition amplitude $W_{fi}(\hat{\mathbf{e}}_S,\hat{\mathbf{e}}_L,\mathbf{q},\mathbf{q}')$. When summing over the whole phonon branch, the integral must be performed only between the origin and the edge of the Brillouin zone to avoid double counting of phonon pairs. The calculation yields a diagonal tensor and the scattering efficiency [Eq. (5)]

$$\left.\frac{dS}{d\Omega}\right|_{2LO}=\frac{32f^2}{3\pi^4}\left[\frac{\omega_S}{\omega_L}\right]^2\left[\frac{n_S}{n_L}\right]\left[\frac{e}{mc}\right]^4 P^4C_F^4 \times\frac{1}{(\hbar\Omega_{LO})^6a_0^2a^{*4}} \times\int_0^\infty q_\perp dq_\perp B(q_\perp)\,|\,Y(a^*q_\perp)\,|^2 . \quad (34)$$

The functions $B(q_\perp)$ and $Y(a^*q_\perp)$ are given in the Appendix. Equation (34) depends on energy through the dimensionless quantities α, β [Eq. (18)], and γ,

$$\gamma=\alpha-2=\frac{\hbar\omega_L-E_1+i\eta^+-2\hbar\Omega_{LO}}{\hbar\Omega_{LO}} . \quad (35)$$

Figure 6 depicts the results of calculations with Eqs. (34), (A3), and (A7) for parameters appropriate to the E_1 gap of GaSb. For very small η three peaks are seen at $\hbar\omega_L=E_1$, $E_1+\hbar\Omega_{LO}$, and $E_1+2\hbar\Omega_{LO}$. In the 3D case, only one peak is seen at the outgoing resonance (Fig. 3 of Ref. 5). This difference results from the divergence of the Green's function for uncorrelated *e-h* pairs (logarithmic singularity) at a 2D electronic critical point. No such divergence occurs in the three-dimensional case. As for impurity-induced scattering, the double resonances are strongly affected by the broadening. At $\eta=40$ meV (the value assumed for the E_1 gap of GaSb) only one maximum is seen, close to $E_1+2\hbar\Omega_{LO}$.

B. Interference effects of plasmons and LO phonons

The same final state is reached for electro-optic (EO) and Fröhlich *intraband* Raman scatttering by plasmons, since the **q** vector of this process is fixed ($\mathbf{q}=\mathbf{k}_L-\mathbf{k}_S$). This also holds for the deformation-potential (and EO) and F-induced (and E-induced) scattering by LO phonons. These processes are mutually coherent. As a consequence the Raman tensors must be added before squaring. The impurity-induced Raman scattering by LO phonons is incoherent with the DP and F mechanism since it leads to a manifold of final states in **q** space. It simply adds intensity to the previous intrinsic mechanisms. For backscattering configurations on a (001) face (Sec. II) we thus get the following scattering efficiencies (to numerical factors different for plasmons and LO phonons):[2]

Configuration	Plasmon	LO phonon
(I) $\bar{z}(x',x')z$	$\lvert a_{EO}+a_F\rvert^2$	$\lvert a_{DP}+a_F\rvert^2+\lvert a_{Fi}\rvert^2$
(II) $z(y',y')z$	$\lvert a_{EO}-a_F\rvert^2$	$\lvert a_{DP}-a_F\rvert^2+\lvert a_{Fi}\rvert^2$
(III) $\bar{z}(x,x)z$	$\lvert a_F\rvert^2$	$\lvert a_F\rvert^2+\lvert a_{Fi}\rvert^2$
(IV) $\bar{z}(y,x)z$	$\lvert a_{EO}\rvert^2$	$\lvert a_{DP}\rvert^2$

We thus expect different scattering intensities by plasmons (and LO phonons) for polarization along $\hat{\mathbf{x}}'=(1/\sqrt{2})\,(1,1,0)$ and $\hat{\mathbf{y}}'=(1/\sqrt{2})\,(\bar{1},1,0)$.

Scattering at the opposite face $(00\bar{1})$ changes only the sign of a_F [because of the factor $\hat{\mathbf{e}}\cdot\mathbf{q}$ in Eq. (21)] for plasmons and LO phonons. The constructive interference becomes destructive and vice versa. At the same time, one may interchange $\hat{\mathbf{x}}'$ and $\hat{\mathbf{y}}'$ and the interference should remain unchanged ([001] is a fourfold improper rotation axis of the T_d group).

The same happens for an interchange of the cation and anion within the PC. In the case of plasmons a_{EO} reverses sign due to the product $PP'Q$, while a_F (C_F) does not. In the case of LO phonons a_F changes sign, due to the change of C_F, while neither a_{DP} nor a_{EO} do so ($C_F PP'Q$ remains unchanged). Thus the interference pattern reverses sign: The interference effects in Raman scattering do not depend on the definition of the primitive cell.

IV. RESULTS AND DISCUSSION

Figures 7 and 8 display Raman spectra (for $\Delta\tilde{\nu}$ between 100 and 800 cm^{-1}) obtained in the four different backscattering configurations (given in the above table) for two different laser energies $\hbar\omega_L$. The plasmon and the LO phonon are clearly observed (the vertical scale of the LO-phonon line has been increased by eight in both figures). There is a dipole-allowed (EO) contribution to the Raman scattering by plasmons (Fig. 7, configuration IV). The $\bar{z}(x',x')z$ configuration (I) yields a spectrum different from that of the $\bar{z}(y',y')z$ configuration (II), revealing that an interference in scattering cross sections occurs. The interference between dipole-allowed and dipole-forbidden Raman scattering is constructive for plasmons in configuration I and for LO phonons in configuration II at $\hbar\omega_L=2.161$ eV. It is interesting to note that the Raman scattering by plasmons vanishes in the $\bar{z}(y',y')z$ configuration (II). This leads us to conclude that no incoherent Raman scattering process is operative for plasmons (at this laser energy), contrary to the case of LO phonons. When one crosses the E_1 gap with the laser ($\hbar\omega_L=2.269$ eV, Fig. 8), the features attributed to the plasmon become weaker with respect to the LO phonon due to increasing absorption. The intensity of the plasmon becomes nearly the same in all configurations, whereas the interference persists for the LO phonon at $\hbar\omega_L=2.269$ eV.

The upper parts of Figs. 9 and 10 [parts (a) and (b)] summarize the resonance profiles measured for plasmons and LO phonons, respectively. The data have been converted into squared Raman polarizabilities as discussed in Sec. II [Eqs. (3) and (4)]. The lines are drawn as a guide for the eye. The error in the absolute squared Ra-

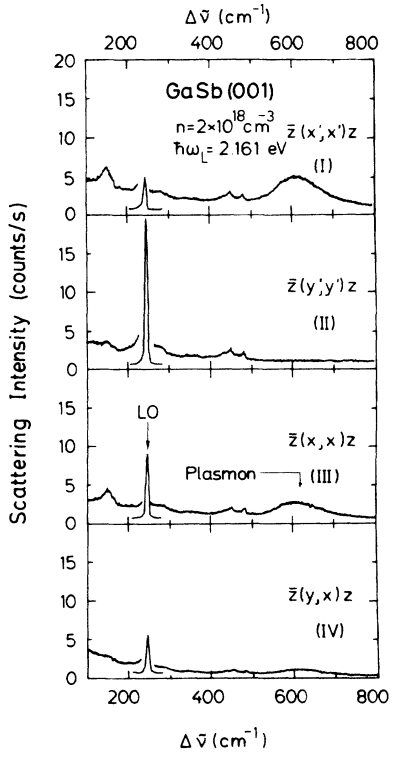

FIG. 7. Raman spectrum between $\Delta\tilde{\nu}=100$–800 cm^{-1}, taken at $\hbar\omega_L=2.161$ eV in the four different backscattering configurations (see table in text, Sec. III B). The vertical scale must be multiplied by eight for the LO phonons.

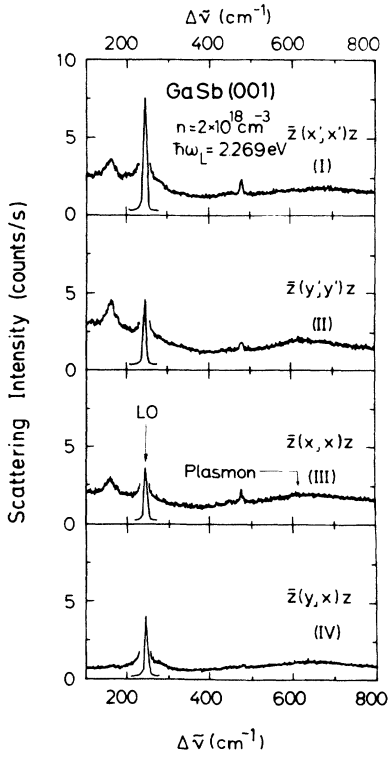

FIG. 8. Raman spectrum between $\Delta\tilde{\nu}=100$–800 cm^{-1}, taken at $\hbar\omega_L=2.269$ eV in the four different backscattering configurations (see table in text, Sec. III B). The vertical scale must be multiplied by eight for the LO phonons.

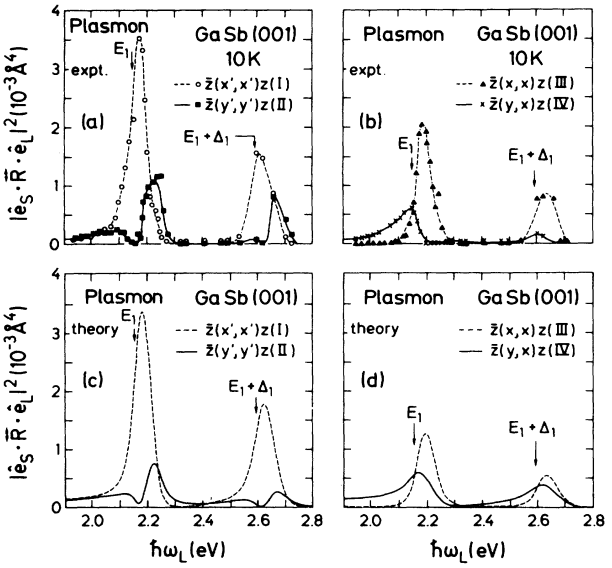

FIG. 9. Resonance profile for Raman scattering by plasmons near the E_1 and $E_1+\Delta_1$ gaps of GaSb. (a) and (b): Experimental points displayed as squared Raman polarizabilities determined in the four different backscattering configurations (see table in text, Sec. III B). The lines are drawn as a guide for the eye. (c) and (d): Calculation with the expressions of Sec. III, assuming q-dependent Fröhlich-induced and electro-optic Raman scattering.

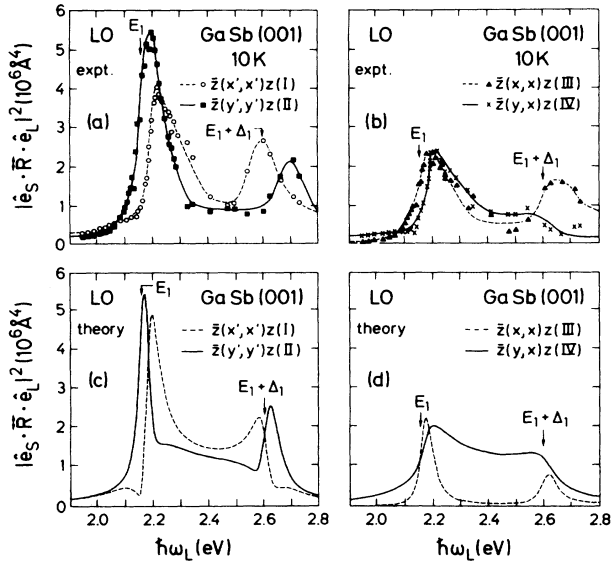

FIG. 10. Resonance profile for Raman scattering by LO phonons near the E_1 and $E_1+\Delta_1$ gaps of GaSb. (a) and (b): Experimental points displayed as squared Raman polarizabilities determined in the four different backscattering configurations (see table in text, Sec. III B). The lines are drawn as a guide for the eye. (c) and (d): Calculation with the expressions of Sec. III and the Appendix, assuming deformation-potential, q-dependent Fröhlich-induced and impurity-induced Raman scattering.

man polarizabilities amounts to about 50%, mainly due to the uncertainty in the Raman polarizability of Si and to the absorption correction near the E_1 and $E_1+\Delta_1$ gaps. The resonance maximum of the constructive interference for plasmons (configuration I) corresponds to the squared Raman polarizability $|\hat{e}_S\cdot\vec{R}\cdot\hat{e}_L|^2=3.5\times10^{-3}$ Å^4 or to the scattering efficiency $dS/d\Omega|_P=9.6\times10^{-2}$ sr^{-1} cm^{-1} [Eqs. (5) and (6)], whereas the corresponding values for LO phonons (configuration II) amount to $|\hat{e}_S\cdot\vec{R}\cdot\hat{e}_L|^2=5.4\times10^6$ Å^4 or $dS/d\Omega|_{LO}=2.2\times10^{-2}$sr^{-1}cm^{-1}. After the correction for absorption, the plasmon and the LO-phonon signals are comparable, and the different scaling factors in Figs. 9 and 10 are due to the difference in the LO-phonon and plasmon amplitude [Eqs. (7) and (8)].

At the E_1 gap, the interference for the $\bar{z}(x',x')z$ configuration (I) is constructive for plasmons, whereas it is destructive for LO phonons. At the $E_1+\Delta_1$ gap this interference remains constructive for plasmons, while it becomes also constructive for LO phonons. This fact has already been accounted for by the theory (Sec. III). The (F) q-dependent scattering is a two-band term which does not change its sign from E_1 to $E_1+\Delta_1$. The EO Raman scattering by plasmons behaves in the same way since it is a three-band mechanism involving a higher conduction band. The dipole-allowed Raman scattering by LO phonons changes its sign from E_1 to $E_1+\Delta_1$. This is true only for the three-band DP scattering (deformation potential $d^5_{3,0}$), which predominates over the two-band ($d^5_{1,0}$) and EO contributions. The observation justifies *a posteriori* the assumptions made in Sec. III A 4. It is confirmed by the fact that the DP scattering by LO phonons is rather strong between the E_1 and $E_1+\Delta_1$ gaps: the three-band terms are still active. The EO scattering by plasmons is stronger on the low-energy side of each gap, whereas on the high-energy side it can hardly be distinguished from the background.

The lower parts [(c) and (d)] of Figs. 9 and 10 display calculations according to the theory developed in Sec. III. The material parameters which were used are listed in Table I.[65,66] The parameters of the gaps were taken from the line-shape analysis of ellipsometric data (Sec. II).

Simulations of the measured resonant interference curves of plasmons are obtained with Eqs. (19) and (23), including in the response function the finite width of the plasmon ($2\hbar\Gamma_P=13$ meV). A real constant added to the Raman polarizability a_{EO} due to the EO mechanism accounts for contributions of different gaps situated away from resonance ($C=-7.6\times10^{-3}$ Å^2). It causes this contribution to be stronger at low energy than at the high-energy side of each gap. The calculations represent the observed features rather well. A completely destructive interference (configuration II) is obtained at $\hbar\omega_L=2.16$ eV. The real and imaginary parts of the calculated Raman tensor a_{EO} and a_F are displayed in Fig. 11. The observed signs at E_1 and $E_1+\Delta_1$ are those predicted by theory.

The interference curves of the LO phonons were calculated with Eqs. (23), (29), (33), (A2), and (A6). For the impurity-induced scattering, the widths of the corre-

TABLE I. Parameters of GaSb used to fit the experimental resonance curves with theoretical expressions.

$E_1 = 2.160$ eV[a]	$\eta^+ = 29.2$ meV[a]
$E_1 + \Delta_1 = 2.597$ eV[a]	$\eta^- = 40.8$ meV[a]
$A^+ = 0.54$ eV[a]	$d^5_{1,0} = -10$ eV
$A^- = 0.54$ eV[a]	$d^5_{3,0} = 60$ eV
$\bar{E}'_1 = 5.6$ eV[b]	$P = 9.5 \times 10^{-8}$ eV cm[c]
$p' = -3.3 \times 10^{-8}$ eV cm[c]	$Q = 8.1 \times 10^{-8}$ eV cm[c]
$\hbar\Omega_P = 75$ meV	$\hbar\Omega_{LO} = 29.5$ meV
$2\hbar\Gamma_P = 13$ meV	$a^* = 44$ Å
$a_0 = 6.09$ Å	$C_{F,LO} = 1 \times 10^{-5}$ eV cm$^{1/2}$
$C_{F,P} = 6.95 \times 10^{-5}$ eV cm$^{1/2}$	$m_{h\perp}^+ = 0.22$ m[d]
$m_{e\perp} = 0.09$ m[d]	$m_{h\perp}^- = 0.28$ m[d]
$M^* = 81\,395$ m	$q_F = 4 \times 10^6$ cm^{-1}[f]
$q = 1.1 \times 10^6$ cm^{-1}[e]	

[a]From ellipsometry.
[b]$\bar{E}'_1 \cong E'_1 + \Delta'_1/2$ (Ref. 65).
[c]Reference 66.
[d]From $\mathbf{k}\cdot\mathbf{p}$ expressions (Ref. 55).
[e]At $\hbar\omega_L = 2.16$ eV, $q = (n_L\omega_L + n_S\omega_S)/c$.
[f]$q_F = 2(4\pi n_I/3)^{1/3}$.

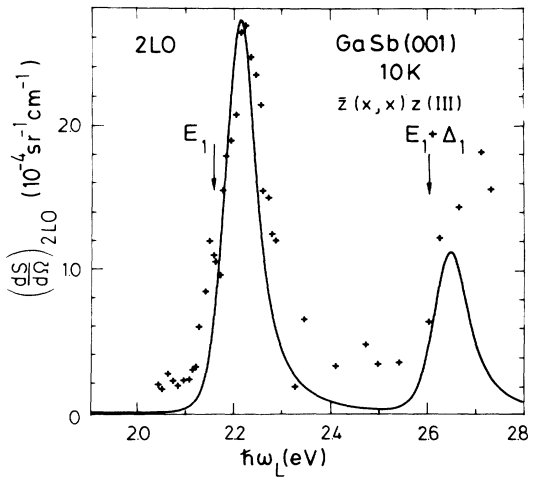

FIG. 12. Raman scattering efficiency for two-LO-phonon scattering near the E_1 and $E_1+\Delta_1$ gaps of GaSb. The lines represent the theoretical fit to the experimental points.

sponding gaps were increased by 10 meV, so as to simulate the slope of the bands in the Λ direction. The adequacy of this approximation can be checked for the resonance of the 2LO-phonon scattering as shown in Fig. 12. The solid line represents the result of a calculation with Eqs. (34), (A3), and (A7) and the parameters of Table I (the broadening of the gap was chosen 10 meV higher). Although there are differences at the high-energy side of the E_1 gap and at $E_1+\Delta_1$, probably due to the absorption corrections, the agreement is remarkable. The theoretical expression yields a scattering efficiency $dS/d\Omega\,|_{2LO} = 9 \times 10^{-5}$ sr^{-1}cm^{-1}, while 2.7×10^{-4}sr^{-1}cm^{-1} is found experimentally. It is at least 2 orders of magnitude lower than the LO-phonon or plasmon signal ($dS/d\Omega = 10^{-1} - 10^{-2}$ sr^{-1}cm^{-1}). The fit of the dipole-allowed scattering by LO phonons with Eq. (29) required $B = 0$ and the deformation potentials $d^5_{1,0} = -10$ eV and $d^5_{3,0} = 60$ eV. The value $d^5_{3,0} + (1/2\sqrt{2})d^5_{1,0} = 56$ eV is in surprisingly good agreement with that found experimentally (53 eV) from the extrapolation of dipole-allowed scattering by LO phonons near the $E_0+\Delta_0$ gap (≈ 1.6 eV).[6] The high value of $d^5_{3,0}$ implies that the three-band contributions to DP scattering by LO phonons are important. In InSb, lower values were determined experimentally around E_1 ($d^5_{3,0} = 33 \pm 8$ eV, $d^5_{1,0} = -16 \pm 4$ eV).[8] Pseudopotential calculations for InSb and Ge yield $d^5_{3,0} \cong 40$ eV and $d^5_{1,0} \cong -20$ eV.[35,67] The results seem to indicate that three-band contributions to DP scattering are more important in GaSb than, e.g., in InSb or Ge. Figure 13 depicts the Raman polarizabilities for DP and F $\mathbf{q}$-induced Raman scattering by LO phonons as a function of laser energy. The real part of a_{DP} changes its sign from E_1 to $E_1+\Delta_1$. Between the gaps, the imaginary part is dominant. The observed signs of the components of a_{DP} and a_F at E_1 and $E_1+\Delta_1$ are those predicted by theory.

The intrinsic contribution (F) to the total dipole-forbidden Raman scattering by LO phonons is obtained from the calculation of Fig. 10(d), evaluated at the resonance maximum. We find

$$|a_F|^2_{max}/(|a_F|^2_{max} + |a_{Fi}|_{max})^2 = 0.7$$

with $|a_F|^2 = 2.4\,|a_{Fi}|^2$. This result differs from earlier observations for InSb.[8] Near the E_1 gap of undoped InSb most of the dipole-forbidden Raman scattering by LO phonons (>90%) was found to be induced by impurities and only a weak interference between the dipole-forbidden and dipole-allowed scattering was seen.[8] The present result differs also from observations on III-V compounds near the $E_0+\Delta_0$ gap, where only less than

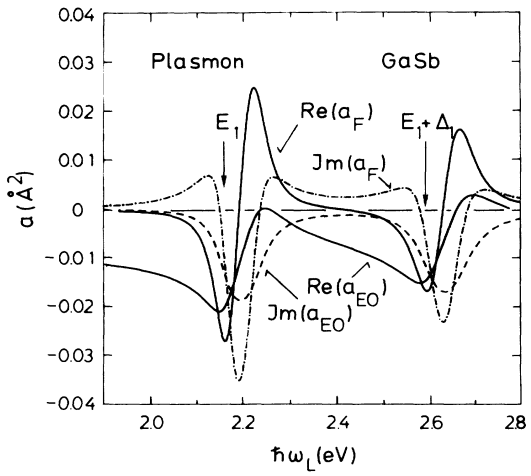

FIG. 11. Energy dependence of the Raman polarizabilities a_{EO} for electro-optic scattering and a_F for $\mathbf{q}$-dependent forbidden scattering by plasmons as used for the calculation of Fig. 9.

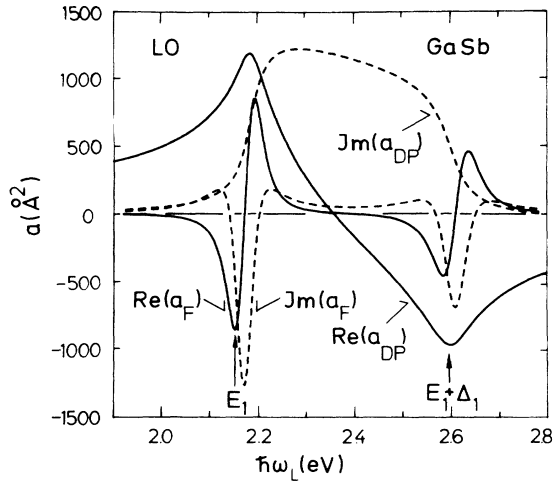

FIG. 13. Energy dependence of the Raman polarizabilities a_{DP} for deformation-potential scattering and a_F for **q**-dependent forbidden scattering by LO phonons as used for the calculation of Fig. 10.

43% of the dipole-forbidden scattering is due to the **q** dependent F-coupling.[2,3,5,6] The high rate of coherent dipole-forbidden scattering by LO phonons can only partly be explained by the suppression of impurity-induced scattering by the large broadening of the E_1 gap, since this argument should also apply to InSb.[8]

In the present case, the dipole-forbidden scattering by LO phonons may be strongly enhanced by the **E**-induced mechanism. In order to check this suggestions, we compare the Raman polarizabilities calculated from the expressions of Sec. III with the prefactors required for the calculations of Figs. 9 and 10, which roughly fit the experimental results. The theoretical prefactors are 6 times lower for a_{EO} and 12 times lower for a_F in the case of plasmon scattering. The calculated F-induced scattering by LO phonons must be increased by 20, while the DP requires only a scaling factor of 1.5 in order to fit the data. The latter lies within the errors in the absorption corrections and the separation of the L_--LO-mode combined feature. The calculated impurity-induced scattering by LO phonons, however, is 80 times larger for $n_I \cong 2\times 10^{18}$ cm^{-3} than the experimental one. The explanation of this fact probably lies in the simplification of the integral over $K_\parallel$.

We note that the scattering mechanisms related to the Fröhlich field of longitudinal excitations (LO phonons, plasmons) appear stronger in the experiment than in the calculations (nearly an order of magnitude). This may be due to the electron-hole correlation (excitons) in the intermediate states: electric fields should strongly affect excitons (autoionization). On the other hand, the high amount of coherent dipole-forbidden scattering by LO phonons near the E_1 gap of *n*-type GaSb can be explained by the scattering induced by the surface field. According to Eq. (26), the Raman polarizability a_E of **E**-induced scattering should be about 7 times larger near resonance than that of the **q**-dependent F scattering a_F for the material parameters of GaSb in Table I. The enhancement factor depends on the average electric field $|\mathbf{E}|$ in the scattering region. Our estimate is based on the reasonable value $E = 1\times 10^5$ V/cm.

The Raman polarizability a_{EO} for EO scattering by plasmons describes a three-wave mixing process:[23] The electric field of the incident light (frequency ω_L) is mixed with the electric field of the created plasmon (frequency $-\Omega_P$) to yield the scattered electrical field (ω_S). We can relate the Raman polarizability to the second-order susceptibility describing the three-wave mixing $\chi^{(2)}_{123}(\omega_L,-\Omega_P,\omega_S)$. Using Eq. (3) of Ref. 36 we obtain[22]

$$a_{EO}=(m_e V_c V)^{1/2}\frac{\partial\chi_{12}}{\partial E_P}\frac{\partial E_P}{\partial Q_3}\ . \tag{36}$$

In Eq. (36), m_e is the effective electron mass at the Γ point, χ_{12} the dielectric susceptibility, E_P the electric field associated with the plasmon, and Q_3 the normal-mode coordinate. The derivative $\partial E_P/\partial Q_3$ is equal to $C_F(2\Omega_P/V\hbar)^{1/2}/e$, and $\partial\chi_{12}/\partial E_P$ is the second-order susceptibility $\chi^{(2)}_{123}$ which is related to a_{EO} through[23]

$$\chi^{(2)}_{123}(\omega_L,-\Omega_P,\omega_S)=\frac{e\hbar^{1/2}}{2^{3/2}C_F\Omega_P^{1/2}V_c^{1/2}m_e^{1/2}}a_{EO}\ . \tag{37}$$

A factor of 2 has been introduced in the denominator of Eq. (37) in order to conform with the usual definition of $\chi^{(2)}_{123}$ in nonlinear optics.[23] Figure 14 displays the dispersion of the second-order susceptibility (in esu) near the E_1 and $E_1+\Delta_1$ gap of GaSb. $\chi^{(2)}_{123}$ has imaginary parts close to the gaps. At resonance near E_1, $|\chi^{(2)}_{123}|$ becomes of the order of 2×10^{-4} esu (6.7×10^{-9} m/V).

An important part of the work on nonlinear susceptibility deals with the second-harmonic generation (SHG) $[\chi^{(2)}_{123}(\omega,\omega,2\omega)]$ (Refs. 68, and 69) or with the EO coefficient $[\chi^{(2)}_{123}(\omega,0,\omega)]$ (Refs. 25 and 69), which give the birefringence induced by a static electric field. Experimental determinations of EO coefficients are usually

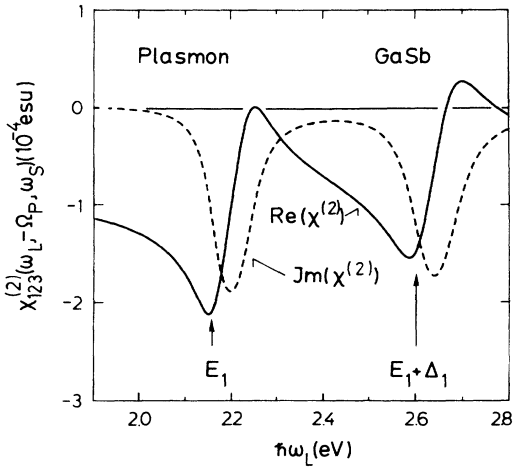

FIG. 14. Dispersion of the second-order nonlinear electric susceptibility $\chi^{(2)}_{123}(\omega_L,-\Omega_P,\omega_S)$ near the E_1 and $E_1+\Delta_1$ gaps of GaSb.

restricted to the spectral region below or close to the lowest absorption edge.[25,26] Measurements and calculations for III-V compounds show that the nonlinear susceptibilities resonate when the sum frequency ω_3 of ω_1 and ω_2 in $\chi^{(2)}_{123}(\omega_1,\omega_2,\omega_3)$ equals the E_1 or $E_1+\Delta_1$ gap.[24,68] For ω_3 close to the E_1 and $E_1+\Delta_1$ gaps, the nonlinear susceptibilities $\chi^{(2)}_{123}$ for SHG are of the order of 3×10^{-6} esu (10^{-16} m/V), 2 orders of magnitude lower than our result which corresponds to $\chi^{(2)}_{123}(\omega_1,0,\omega_3)$. The latter would be expected to be larger than the former, since it has two energy dominators fulfilling the resonance condition instead of one.[68] The measurement of the EO scattering by plasmons and their interference with F-induced Raman scattering near critical points provides a tool to determine the dispersion of nonlinear susceptibilities and to separate their real and imaginary parts.

Measurements of the Faust-Henry coefficient by Raman scattering have also been used to determine the EO coefficient below the fundamental absorption edge in the long-wavelength limit [Eq. (28)].[69,70] In the fundamental absorption region C, defined as[22]

$$C=\frac{e_T}{M^*\Omega_{\rm TO}^2}\left[\frac{\partial\chi_{12}/\partial u}{\partial\chi_{12}/\partial E}\right], \tag{38}$$

becomes complex. $\partial\chi_{12}/\partial u$ is the susceptibility associated with DP scattering. It is then not possible to determine the Faust-Henry coefficient C (real and imaginary parts) from the measured ratio $|a_{\rm LO}/a_{\rm TO}|^2$. A complex C, as determined from the calculations of Fig. 13 for LO phonons ($\partial\chi_{12}/\partial u$) and from Fig. 14 for plasmons ($\partial\chi_{12}/\partial E$) can, however, be used to predict the ratio $|a_{\rm LO}/a_{\rm TO}|^2$ [Eq. (28)]. We determine this ratio by measuring the dipole-allowed scattering by TO phonons in backscattering on a (111) face of a similar sample (crossed polarization) and comparing the result for LO-phonon dipole-allowed scattering in a spectral region where the signal is essentially confined to the surface depletion layer ($\hbar\omega_L\geq2.4$ eV). We obtained $|a_{\rm LO}/a_{\rm TO}|^2=1.3\pm0.1$, nearly independent of laser frequency. The value estimated from the calculated dispersion of $\chi^{(2)}_{123}$ and $a_{\rm DP}$ (Figs. 13 and 14) is $|a_{\rm LO}/a_{\rm TO}|^2=1.1$ at $\hbar\omega_L=2.4$ eV and $|a_{\rm LO}/a_{\rm TO}|^2=1.4$ at $\hbar\omega_L=2.5$ eV. Thus the $|a_{\rm LO}/a_{\rm TO}|$ ratio should, in general, not be constant over the spectral range due to the different dispersion of the Raman tensor of DP and EO scattering. The complex Faust-Henry coefficient varies from $C=-0.15-i0.6$ at $\hbar\omega_L=2.4$ eV to $C=-0.23-i0.24$ at $\hbar\omega_L=2.5$ eV.

V. CONCLUSION

We have shown that the dipole-allowed (electro-optic) Raman scattering by plasmons interferes with the dipole-forbidden (F induced) one near the E_1 and $E_1+\Delta_1$ gaps. The sign of the interference is predicted by the theory developed and is consistent with that seen for the LO phonon of the surface depletion layer. The absolute values of Raman polarizabilities are in qualitative agreement with those obtained from a theory which assumes uncorrelated e-h pairs: A quantitative comparison suggests that excitonic effects are important near the E_1 and $E_1+\Delta_1$ gaps and that the main part of the dipole-forbidden Raman scattering by LO phonons is due to the electric-field-induced mechanism. The measurement of the resonance of the electro-optic scattering near interband critical points yields information about the dispersion of the nonlinear electric susceptibility (real and imaginary parts) near the corresponding gap.

ACKNOWLEDGMENTS

The authors are indebted to H. Hirt, M. Siemers, and P. Wurster for their technical assistance. We gratefully acknowledge the help of M. Garriga and P. Lautenschlager for performing the ellipsometric measurements and the line-shape analysis.

APPENDIX

The integrals over the electronic density of states ($\mathbf{K}$) and the phonon branch ($\mathbf{q}$) must be carried out in cylindrical coordinates. The wave vector $K_\parallel$ varies from 0 to $\pi\sqrt{3}f/a_0$, where $f\simeq\frac{3}{4}$ is the portion of the Λ direction where the $\Lambda_6^{c,l}$ and $\Lambda_{4,5}^v$ (Λ_6^v) bands are parallel. After the decomposition of the denominator into partial fractions, the integration perpendicular to the [111] direction ($K_\perp$) leads to integrals of the form[35,71]

$$I(-A,B,C)=\int_0^\infty\frac{1}{(x-A)(x^2+2Bx+C^2)^{1/2}}dx$$
$$=\frac{1}{\sqrt{z}}\ln\left[\frac{\sqrt{z}C-C^2-AB}{A(\sqrt{z}+A+B)}\right], \tag{A1}$$

with $z=A^2+2AB+C^2$ and $x=a^{*2}K_\perp^2$.

The integration over $K_\perp$ yields the function $X(a^*q_\perp)$ for impurity-induced scattering and $Y(a^*q_\perp)$ in the case of 2LO-phonon scattering:

$$X(a^*q_\perp)=I(-\alpha,a,b)-I(-\beta,a,b)+I(-\alpha,g,h)-I(-\beta,g,h)+I(-\alpha,c,d)-I(-\beta,c,d)+I(-\alpha,i,j)-I(-\beta,i,j)$$
$$+\frac{1}{s_h-s_es_ha^{*2}q_\perp^2}[s_eI(-\alpha,a,b)-s_eI(-\delta',a,b)-I(-\alpha,k,l)+I(-\delta',k,l)]$$
$$-\frac{1}{s_e+s_es_ha^{*2}q_\perp^2}[s_eI(-\alpha,g,h)-s_eI(-\delta'',g,h)-I(-\alpha,k,l)+I(-\delta'',k,l)]$$
$$+\frac{1}{s_e-s_es_ha^{*2}q_\perp^2}[s_hI(-\alpha,c,d)-s_hI(-\varepsilon',c,d)-I(-\alpha,k,l)+I(-\varepsilon',k,l)]$$
$$-\frac{1}{s_h+s_es_ha^{*2}q_\perp^2}[s_hI(-\alpha,i,j)-s_hI(-\varepsilon'',i,j)-I(-\alpha,k,l)+I(-\varepsilon'',k,l)] \tag{A2}$$

and

$$Y(a^*q_\perp)=\tfrac{1}{2}[I(-\alpha,a,b)-I(-\gamma,a,b)-I(-\gamma,c,d)+I(-\alpha,c,d)]$$
$$+\frac{1}{s_h-s_e-s_es_ha^{*2}q_\perp^2}[s_eI(-\alpha,a,b)-s_eI(-\delta,a,b)-I(-\alpha,e,f)+I(-\delta,e,f)]$$
$$+\frac{1}{s_e-s_h-s_es_ha^{*2}q_\perp^2}[s_hI(-\alpha,c,d)-s_hI(-\varepsilon,c,d)-I(-\alpha,e,f)+I(-\varepsilon,e,f)]\ . \tag{A3}$$

$X(a^*q_\perp)$ and $Y(a^*q_\perp)$ depend on functions of the laser energy through the dimensionless quantities α, β, and γ defined as

$$\alpha=(\hbar\omega_L+i\eta-E_1)/\hbar\Omega_{\rm LO},\quad \beta=\alpha-1,\quad \gamma=\alpha-2\ . \tag{A4}$$

The variables introduced in (A2) and (A3) represent

$$a=-\beta-a^{*2}s_e^2q_\perp^2,\quad b=a+2\beta,\quad c=-\beta-a^{*2}s_h^2q_\perp^2,\quad d=c+2\beta,\quad e=-\gamma-a^{*2}q_\perp^2,\quad f=e+2\gamma\ ,$$
$$g=-\alpha-a^{*2}s_e^2q_\perp^2,\quad h=g+2\alpha,\quad i=-\alpha-a^{*2}s_h^2q_\perp^2,\quad j=i+2\alpha,\quad k=-\beta-a^{*2}q_\perp^2,\quad l=k+2\beta\ ,$$
$$\delta=\beta+\frac{s_e}{s_h}+s_ea^{*2}q_\perp^2,\quad \delta'=\beta+s_ea^{*2}q_\perp^2,\quad \delta''=\alpha+\frac{s_e}{s_h}+s_ea^{*2}q_\perp^2\ , \tag{A5}$$
$$\varepsilon=\beta+\frac{s_h}{s_e}+s_ha^{*2}q_\perp^2,\quad \varepsilon'=\beta+s_ha^{*2}q_\perp^2,\quad \varepsilon''=\alpha+\frac{s_h}{s_e}+s_ha^{*2}q_\perp^2\ .$$

For the integration over the phonon branch $[\mathbf{q}=(q_\parallel,q_\perp)]$ we neglect the dispersion of the LO-phonon energy. The limits of integration for $q_\parallel$ can be set equal to infinity instead of $2\pi/a_0$ without any loss of accuracy. We obtain the functions $A(a^*q_\perp)$ and $B(a^*q_\perp)$ in the case of impurity-induced and 2LO-phonon scattering, respectively:

$$A(a^*q_\perp)=\frac{\pi}{q_F^4}\left[\frac{1}{q_\perp}-\frac{(2q_\perp^2-q_F^2)}{2(q_\perp^2+q_F^2)^{3/2}}\right] \tag{A6}$$

and

$$B(a^*q_\perp)=\frac{\pi}{4q_\perp^3}\ . \tag{A7}$$

[1] J. Menéndez and M. Cardona, Phys. Rev. Lett. **51**, 1297 (1983).
[2] J. Menéndez and M. Cardona, Phys. Rev. B **31**, 3693 (1985).
[3] M. Kauschke, M. Cardona, and E. Bauser, Phys. Rev. B **35**, 8030 (1987).
[4] W. Kauschke, V. Vorlíček, M. Cardona, L. Viña, and W. I. Wang, Solid State Commun. **61**, 487 (1987).
[5] W. Kauschke and M. Cardona, Phys. Rev. B **33**, 5473 (1986).
[6] W. Kauschke and M. Cardona Phys. Rev. B **35**, 9619 (1987).
[7] W. Kauschke, V. Vorlíček, and M. Cardona (unpublished).
[8] J. Menéndez, L. Viña, M. Cardona, and E. Anastassakis, Phys. Rev. B **32**, 3966 (1985).
[9] C. Y. Chen, Phys. Rev. B **27**, 1436 (1983).
[10] A. Mooradian and A. L. McWhorter, in *Light Scattering Spectra of Solids,* edited by G. B. Wright (Springer, Berlin, 1969), p. 297.
[11] M. V. Klein, B. N. Ganguly, and P. J. Colwell, Phys. Rev. B **6**, 2380 (1972).
[12] M. V. Klein, in *Light Scattering in Solids I,* Vol. 8 of *Topics in Applied Phyisics,* edited by M. Cardona (Springer, Berlin, 1975), p. 147.
[13] G. Abstreiter, M. Cardona, and A. Pinczuk, in *Light Scattering in Solids IV,* Vol. 54 of *Topics in Applied Physics,* edited by M. Cardona and G. Güntherodt (Springer, Berlin, 1984), p. 5.
[14] A. Pinczuk, G. Abstreiter, R. Trommer, and M. Cardona, Solid State Commun. **30**, 429 (1979).
[15] S. Buchner and E. Burstein, Phys. Rev. Lett. **33**, 908 (1974).
[16] M. Cardona and G. Harbeke, J. Appl. Phys. **34**, 813 (1963).
[17] B. B. Varga, Phys. Rev. **137**, A1896 (1965).
[18] A. Mooradian and G. B. Wright, Phys. Rev. Lett. **16**, 999 (1966); A. Mooradian and A. L. McWhorter, *ibid.*, **19**, 849 (1967); B. Tell and R. J. Martin, Phys. Rev. **167**, 381 (1968).
[19] G. Abstreiter, R. Trommer, M. Cardona, and A. Pinczuk, Solid State Commun. **30**, 703 (1979).
[20] R. Trommer and A. K. Ramdas, in *Proceedings of the Fourteenth International Conference on the Physics of Semiconductors, Edinburgh, 1978,* edited by B. L. H. Wilson [Inst. Phys. Conf. Ser. No. 43 (IOP, Bristol, 1979)], p. 585.
[21] At $n\cong(1-2)\times10^{18}\text{cm}^{-3}$ some small amount of free carriers occurs near the L point of GaSb, giving rise to new scattering mechanicsms (Refs. 13 and 14). In GaSb and L minima of the conduction band lie only 100 meV above the Γ minimum. For our purpose, we will neglect the influence of the few carriers in L minima on Raman scattering by plasmons.
[22] M. Cardona, in *Light Scattering in Solids II,* Vol. 50 of *Topics in Applied Physics,* edited by M. Cardona and G. Güntherodt (Springer, Berlin, 1982), p. 19.
[23] N. Bloembergen, *Nonlinear Optics* (Benjamin, New York, 1963).
[24] M. I. Bell, in *Electronic Density of States,* Natl. Bur. Stand.

(U. S.) Spec. Publ. No. 323, edited by L. H. Bennett (U. S. GPO, Washington, D.C., 1971), p. 757.

[25]M. I. Bell, in *Proceedings of the Eleventh International Conference on the Physics of Semiconductors, Warsaw, 1972,* edited by M. Miasek (PWN-Polish Scientific, Warsaw, 1972), p. 845.

[26]D. C. Hamilton, Phys. Rev. **188**, 1221 (1969); R. M. Martin and T. C. Damen, Phys. Lett. **26**, 86 (1971); R. M. Martin, Phys. Rev. B **4**, 3676 (1971).

[27]A. A. Gogolin and E. I. Rashba, in *Proceedings of the Thirteenth International Conference on the Physics of Semiconductors,* Rome, 1976, edited by F. G. Fumi (Tipografia Marves, Rome, 1976), p. 284; Solid State Commun. **19**, 1177 (1976).

[28]C. A. Mead and W. G. Spitzer, Phys. Rev. **134**, A713 (1964); R. Manzke, H. P. Barnscheidt, C. Janowitz, and M. Skibowski, Phys. Rev. Lett. **58**, 610 (1987).

[29]G. Abstreiter, A. Pinzuk, R. Trommer, and R. Tsu, in *Proceedings of the Thirteenth International Conference on the Physics of Semiconductors, Rome, 1976,* edited by F. G. Fumi (Tipografia Marves, Rome, 1976), p. 779.

[30]A. Pinczuk, A. A. Ballman, R. E. Nahory, M. A. Pollack, and J. M. Worlock, J. Vac. Sci. Technol. **16**, 1168 (1979); H. Shen, F. H. Pollak, and R. N. Sacks, Appl. Phys. Lett. **47**, 891 (1985); R. Fukasawa, M. Wakaki, K. Ohta, and H. Okumura, Jpn. J. Appl. Phys. **25**, 652 (1986).

[31]W. Richter, R. Zeyher, and M. Cardona, Phys. Rev. B **18**, 4312 (1978).

[32]A. Pinczuk and E. Burstein, Phys. Rev. Lett. **21**, 1073 (1968); in *Light Scattering Spectra of Solids,* edited by G. B. Wright (Springer, Berlin, 1969), p. 429; in *Proceedings of the Twelfth International Conference on the Physics of Semiconductors, Cambridge, Mass., 1970,* edited by S. P. Keller, J. C. Hensel, and F. Stern (U.S. AEC, Oak Ridge, Tenn., 1970), p. 727.

[33]J. G. Gay, J. D. Dow, E. Burstein, and A. Pinczuk, in *Light Scattering in Solids,* edited by M. Balkanski (Flammarion Sciences, Paris, 1971), p. 33.

[34]R. Zeyher, Phys. Rev. B **9**, 4439 (1974).

[35]M. A. Renucci, J. B. Renucci, R. Zeyher, and M. Cardona, Phys. Rev. B **10**, 4309 (1974).

[36]J. Menéndez, M. Cardona, and L. K. Vodopyanov, Phys. Rev. B **31**, 3705 (1985).

[37]R. Trommer and M. Cardona, Phys. Rev. B **17**, 1865 (1978).

[38]F. Cerdeira, W. Dreybrodt, and M. Cardona, in *Proceedings of the Eleventh International Conference on the Physics of Semiconductors, Warsaw, 1972,* edited by M. Miasek (PWS-Polish Scientific, Warsaw, 1972), p. 1142; W. Dreybrodt, W. Richter, F. Cerdeira, and M. Cardona, Phys. Status Solidi B **60**, 145 (1973).

[39]R. L. Farrow, P. C. Black, and R. K. Chang, in *Proceedings of the International Conference on Lattice Dynamics,* edited by M. Balkanski (Flammerion Sciences, Paris, 1979), p. 182; R. L. Farrow, R. K. Chang, and R. M. Martin, in *Proceedings of the Fourteenth International Conference on the Physics of Semiconductors, Edinburgh, 1978,* edited by B. L. H. Wilson [Inst. Phys. Conf. Ser. No. 43 (IOP, Bristol, 1979)], p. 485.

[40]R. Carles, N. Saint-Cricq, J. B. Renucci, A. Zwick, and M. A. Renucci, Phys. Rev. B **22**, 6120 (1980).

[41]P. Y. Yu and Y. R. Shen, Phys. Rev. Lett. **29**, 468 (1972); P. Y. Yu and Y. R. Shen, Solid State Commun. **15**, 161 (1974).

[42]R. M. A. Azzam and N. M. Bashara, *Ellipsometry and Polarized Light* (North-Holland, Amsterdam, 1977), p. 1.

[43]H. J. Mattausch and D. E. Aspnes, Phys. Rev. B **23**, 1896 (1981).

[44]D. E. Aspnes and A. A. Studna, Phys. Rev. B **27**, 985 (1983).

[45]M. Cardona, *Modulation Spectroscopy,* Supplement 11 of *Solid State Physics,* edited by F. Seitz, D. Turnbull, and H. Ehrenreich (Academic, New York, 1969).

[46]D. E. Aspnes in *Handbook on Semiconductors,* edited by M. Balkanski (North-Holland, Amsterdam, 1980), Vol. 2, p. 109.

[47]H. C. Gatos and M. C. Lavine, in *Progress in Semiconductors,* edited by A. F. Gibson and R. E. Burgess (Temple, London, 1965), Vol. 9, p. 1.

[48]C. Firmani, E. Ruiz, C. W. Carlson, M. Lampton, and F. Paresce, Rev. Sci. Instrum. **53**, 570 (1982).

[49]J. Wagner and M. Cardona, Solid State Commun. **48**, 301 (1983).

[50]H. Wendel, Solid State Commun. **31**, 423 (1979).

[51]W. C. Dash and R. Newman, Phys. Rev. **99**, 1151 (1955).

[52]O. Madelung, Festkörpertheorie (Springer, Berlin, 1972), p. 1.

[53]A. Blacha, H. Presting, and M. Cardona, Phys. Status Solidi B **126**, 11 (1984); the choice of atomic positions in the primitive cell in this work is opposite to our definition and implies a change in sign of our matrix elements with respect to this reference.

[54]M. Cardona and F. H. Pollak, Phys. Rev. **142**, 530 (1966); C. W. Higginbotham, F. H. Pollak, and M. Cardona, in *Proceedings of the Ninth International Conference on the Physics of Semiconductors, Moscow, 1968,* (Nauka, Leningrad, 1968), p. 57.

[55]M. Cardona, in *Atomic Structure and Properties of Solids,* Proceedings of the International School of Physics "Enrico Fermi," Course LII, Varenna, 1971, edited by E. Burstein (Academic, New York, 1972), p. 514.

[56]W. Franz, Z. Naturforsch. Teil A **13**, 484 (1958); L. V. Keldysh, Zh. Eksp. Teor. Fiz. **34**, 1138 (1958) [Sov. Phys.—JETP **7**, 788 (1958)].

[57]V. Dvorak, Phys. Rev. **159**, 652 (1967).

[58]P. A. Fleury and J. M. Worlock, Phys. Rev. **174**, 6131 (1968); J. M. Worlock, in *Light Scattering Spectra of Solids,* edited by G. B. Wright (Springer, Berlin, 1969), p. 411.

[59]F. Schäffler and G. Abstreiter, Phys. Rev. B **34**, 4017 (1986).

[60]H. Brugger, F. Schäffler, and G. Abstreiter, Phys. Rev. Lett. **52**, 141 (1984).

[61]K. Kikuchi, K. Tada, and M. Aoki, J. Phys. Chem. Solids **41**, 1361 (1980).

[62]D. E. Aspnes, Surf. Sci. **37**, 418 (1973).

[63]W. L. Faust and C. H. Henry, Phys. Rev. Lett. **17**, 1265 (1966).

[64]E. O. Kane, Phys. Rev. **178**, 1368 (1969).

[65]D. E. Aspnes, C. G. Olson, and D. W. Lynch, Phys. Rev. B **14**, 4450 (1976).

[66]G. Fasol (private communication).

[67]H. Presting, Ph.D. thesis, Universität Stuttgart, 1985 (unpublished); W. Pötz and P. Vogl, Phys. Rev. B **24**, 2025 (1981).

[68]R. K. Chang, J. Ducuing, and N. Bloembergen, Phys. Rev. Lett. **15**, 415 (1965); F. G. Parsons and R. K. Chang, Opt. Commun. **3**, 173 (1971); H. Lotem, G. Koren, and Y. Yacoby, Phys. Rev. B **9**, 3532 (1974); H. Lotem and Y. Yacoby, *ibid.* **10**, 3402 (1974); D. Bethune, A. J. Schmidt, and Y. R. Shen, *ibid.*, **11**, 3867 (1975).

[69]W. D. Johnston, Jr. and I. P. Kaminow, Phys. Rev. **188**, 1209 (1969); W. D. Johnston, Jr., Phys. Rev. B **1**, 3494 (1970).

[70]G. Vergara, C. de las Heras, and F. Meseguer (unpublished).

[71]I. S. Gradshteyn and I. M. Ryzhik, *Table of Integrals, Series, and Products* (Academic, New York, 1965).